Tellus B
Chemical and Physical Meteorology

ISORROPIA-Lite: A Comprehensive Atmospheric Aerosol Thermodynamics Module for Earth System Models

ORIGINAL RESEARCH PAPER

STYLIANOS KAKAVAS
SPYROS N. PANDIS
ATHANASIOS NENES

*Author affiliations can be found in the back matter of this article

STOCKHOLM UNIVERSITY PRESS

CORRESPONDING AUTHORS:

Spyros N. Pandis

Institute of Chemical Engineering Sciences, Foundation for Research and Technology Hellas, Patras, Greece; Department of Chemical Engineering, University of Patras, Patras, Greece

spyros@chemeng.upatras.gr

Athanasios Nenes

Institute of Chemical Engineering Sciences, Foundation for Research and Technology Hellas, Patras, Greece; School of Architecture, Civil and Environmental Engineering, École Polytechnique Fédérale de Lausanne (EPFL), Switzerland

athanasios.nenes@epfl.ch

ABSTRACT

Aerosol simulations especially for Earth System Models require a thermodynamics module with a good compromise between rigor and computational efficiency. We present and evaluate ISORROPIA-lite, an accelerated and simplified version of the widely used ISORROPIA-II v.2.3 aerosol thermodynamics model, expanded to include the effects of water uptake from organics and an updated interface communicating simulation diagnostics and information. ISORROPIA-lite assumes the aerosol is in metastable equilibrium (i.e., salts do not precipitate from supersaturated solutions) and treats the thermodynamics of Na^+–NH_4^+–SO_4^{2-}–NO_3^-–Cl^-–Ca^{2+}–K^+–Mg^{2+}–Organics–H_2O aerosol using binary activity coefficients from precalculated look-up tables. Off-line comparison between ISORROPIA-II and ISORROPIA-lite (without organic water effects) for more than 330,000 atmospherically-relevant states demonstrated that *i*) ISORROPIA-lite provides virtually identical results with ISORROPIA-II in metastable mode and *ii*) differences between stable mode ISORROPIA-II and ISORROPIA-lite are less than 25% for the concentrations of the various semivolatile aerosol components and similar to the differences between stable and metastable modes of ISORROPIA-II. Using ISORROPIA-lite reduced computational cost by 35% compared to ISORROPIA-II simulations in stable mode with online calculation of binary activity coefficients. Application of ISORROPIA-lite in the PMCAMx chemical transport model accelerated the 3D simulations by about 10% compared to using ISORROPIA-II in stable mode with changes in the concentrations of the major aerosol components of less than 10%. Simulations considering the effects of the organic aerosol water did not slow down ISORROPIA-lite but increased the concentrations of the inorganic semivolatile components especially at nighttime. Organic water could highly contribute to the total PM_1 water mass and increase the concentrations of fine nitrate and ammonium by as much as 1 μg m^{-3} in places where the organic aerosol and RH levels are high.

KEYWORDS:
aerosol thermodynamics; metastable state; nitrate; ammonium; organic water

TO CITE THIS ARTICLE:
Kakavas, S, Pandis, SN and Nenes, A. (2022). ISORROPIA-Lite: A Comprehensive Atmospheric Aerosol Thermodynamics Module for Earth System Models. *Tellus B: Chemical and Physical Meteorology*, 74(2022), 1–23. DOI: *https://doi.org/10.16993/tellusb.33*

1. INTRODUCTION

Atmospheric particulate matter (PM) is composed of inorganic salts, organic compounds and elemental carbon, oxides of trace metals, crustal material and water. Inorganic salts often constitute 50% or more of fine particulate matter (particles with diameter less than 2.5 μm) with sulfate (SO_4^{2-}), bisulfate (HSO_4^-), ammonium (NH_4^+), nitrate (NO_3^-), chloride (Cl^-) and sodium (Na^+) ions being the dominant ones (Heitzenberg, 1989; Fountoukis and Nenes, 2007). Additionally, the potassium cation, K^+, often dominant in the fine aerosol mode in case of biomass burning events, was used in the study of Metzger et al. (2006), who investigated the importance of mineral cations and organic acids in the gas-aerosol partitioning of reactive nitrogen compounds. Dust components such as Ca^{2+}, and Mg^{2+} together with hygroscopic sea salt (Na^+, Cl^-) are found mainly in the coarse PM fraction. The inorganic fraction is often responsible for most of the water uptake by fine PM and therefore for a large fraction of the interactions between aerosols and atmospheric radiation (Burgos et al., 2019). The inorganic fraction largely controls the aerosol pH, which together with aerosol water determine the sensitivity of PM to precursor emissions, chemical reaction rates (Tilgner et al., 2021) and shape the many impacts aerosol has on climate, public health and ecosystem productivity (Pye et al., 2020; Baker et al., 2021).

Computing the phase state and composition of aerosols in thermodynamic equilibrium is a complex computational problem, because it involves the solution of a system of several nonlinear algebraic equations or the minimization of the free energy of the gas-particle system (Nenes et al., 1999). Several thermodynamic equilibrium models have been developed over the last four decades, treating different sets of aerosol components and using different thermodynamic and numerical approaches. Characteristic examples include EQUIL (Basset and Seinfeld, 1983), SEQUILIB (Pilinis et al., 1987), SCAPE2 (Kim and Seinfeld, 1995; Meng et al., 1995), ISORROPIA (Nenes et al., 1998), EQUISOLV II (Jacobson, 1999), GFEMN (Ansari and Pandis, 1999a, b), AIM2 (Wexler and Clegg, 2002), EQSAM (Metzger et al., 2002a, b), UHAERO (Amundson et al., 2006), ISORROPIA-II (Fountoukis and Nenes, 2007), and EQSAM4clim (Metzger et al., 2016).

One of the most important challenges that thermodynamic models face regards the phase diagram used to determine the possible species present. Typically models either allow for salts to precipitate out of solution when supersaturated ("stable solution") or allow salts to remain in-solution even if supersaturated ("metastable solution"). These two treatments give identical solutions when the humidity exceeds the deliquescence point of the major salts in solution (typically ammonium nitrate and sulfate, i.e., around 70%), while the two solutions increasingly diverge as humidity levels decrease. The metastable equilibrium solution leads to higher concentrations of aerosol water compared to stable aerosol, especially at intermediate humidity levels (30–70%). This in turn affects the size, lifetime (e.g., Song et al., 2019) and scattering efficiency of particles (e.g., Bougiatioti et al., 2016). Observations suggest that metastable states may be ubiquitous in aerosol (e.g., Rood et al., 1989; Tang et al., 1995), as aerosol liquid water and semi-volatile partitioning of ammonia and nitrate is consistent with metastable states down to 40% RH in many field observations (Guo et al., 2015; Bougiatioti et al., 2016; Guo et al., 2018). The presence of multiple dissolved salts and organic species depresses the water activity in aerosol, forming eutectic mixtures that can be thermodynamically stable at much lower humidity than expected from the deliquescence humidity of each of the individual components in the aerosol (Brooks et al., 2002; Bertram et al., 2011; Peckhaus et al., 2012). This phenomenon, known as "mutual deliquescence" (Wexler and Seinfeld, 1991), can greatly promote the presence of thermodynamically stable water in aerosol down to low RH and tends to support a "metastable-like" liquid water content and thermodynamic state (Brooks et al., 2003; Parsons et al., 2004).

Organic aerosol, although less hygroscopic than inorganic aerosol, could also contribute significantly to the total aerosol water (Guo et al., 2015; Bougiatioti et al., 2016; Jathar et al., 2016; Jin et al., 2020). This aerosol water due to the organics further promotes a "metastable-like" aerosol state. Furthermore, the added water can induce secondary inorganic aerosol formation since the additional water mass drives more of the gas phase components to partition to the aerosol to satisfy equilibrium (e.g., Ansari and Pandis, 2000a). These feedbacks are usually not treated in thermodynamic modules and are not considered in chemical transport models.

While adoption of thermodynamic modules at present is standard for all regional chemical transport models, they are not included in many of the Earth System Models used in the IPCC or other assessments. For example, EC-Earth (Hazeleger et al., 2011) and ECHAM (Roeckner et al., 2003) do not simulate aerosol thermodynamics, while NorESM (Bentsen et al., 2013; Iversen et al., 2013) uses a zeroth-order estimate for aerosol nitrate formation (Kirkevåg et al., 2013). ESMs could benefit from the improved simulation of aerosol thermodynamics, as simplified parameterizations of nitrate uptake and hygroscopicity may lead to errors in simulated light scattering and associated climate forcing (Burgos et al., 2020). Metzger et al. (2018) also pointed out the importance of aerosol water for climate studies.

Part of the delay to adopt thermodynamic modules in ESMs is related to their complex model development cycle (NRC, 2012). Computational time is another

important factor as thermodynamic calculations need to be repeated millions or even billions of times in such frameworks and can significantly increase their computational burden. The first generations of aerosol thermodynamics models paid little attention to computational efficiency, and were too expensive for use in 3D frameworks. Subsequent efforts however improved solution algorithms and simplified calculations so that modules were fast enough to enable their integration in 3D frameworks. ISORROPIA-II (Fountoukis and Nenes, 2007) is, together with EQSAM, one of the most widely used thermodynamic modules currently, largely because it provides a good balance between comprehensive treatment of inorganic aerosol thermodynamics and simplifications and algorithms that are computationally efficient. Furthermore, ISORROPIA-II can consider the major inorganic ions present in aerosol, treat both stable and metastable states and solve for two classes of problems: the gas-phase equilibrium partitioning ("forward") problem, and the equilibrium vapor pressure calculation ("reverse") problem, based on aerosol composition alone. The latter is needed when long equilibration timescales demand explicit dynamic mass transfer calculations between the aerosol and gas phases (Capaldo et al., 2000; Pilinis et al., 2000; Kakavas et al., 2021).

Despite the previous efforts to produce both accurate and computational efficient aerosol thermodynamics modules, additional improvements are desired to increase their suitability for the computationally demanding long simulations of ESMs. One approach is to simplify the phase diagram, assuming that the aerosol is always in metastable state, especially given the observational support to date. This assumption may speed up calculations at intermediate RH, where the precipitation of salts out of supersaturated aerosol requires the expensive solution of multiple equations. Also, at lower RH, where there is lack of an aqueous phase, the simulation surface of solid aerosols is discontinuous which may cause numerical instabilities in the host model. Although stable aerosol may exhibit higher concentrations of aerosol ammonium and nitrate at humidity below 50% (Ansari and Pandis, 2000b; Moya et al., 2007; Fountoukis et al., 2009), aerosol-gas partitioning may be somewhat insensitive to the actual phase state at intermediate to low RH in most of the atmosphere, given that the nitrate partitioning strongly shifts to the aerosol phase at low temperatures (Guo et al., 2017). This is supported by Karydis et al. (2016), who showed with the EMAC global model that the tropospheric burden of nitrate aerosol decreases by just 2% when the aerosol is assumed to be in a metastable state.

All the above suggest that simplified thermodynamic modules which assume metastable aerosol may be an appropriate choice for ESMs and CTMs. Towards this, Metzger et al. (2016) developed the EQSAM4clim module based on parameterizations that eliminate the need for iterations. Replacing ISORROPIA with EQSAM4clim in CAMx, Koo et al. (2020) reported a reduction in computational time by 4% during winter and 7% during summer assuming metastable aerosols.

We build upon these findings and test whether assuming metastable aerosol and other simplifications in ISORROPIA-II can accelerate the calculations of 3D models without substantial impacts on their results. From these efforts, a new thermodynamics module, ISORROPIA-lite is developed that solves only the metastable state problem and always uses pre-calculated tables of binary activity coefficients to boost computational efficiency. It also simulates the effects of the organic aerosol water in the partitioning of the inorganic components. The predictions of ISORROPIA-lite are first compared against the predictions of ISORROPIA-II in stable mode (with the complete activity coefficient module), without organic aerosol water effects. Evaluations involve differences in predicted composition and computational cost, and are carried out off-line and in the chemical transport model PMCAMx. Then the effect of organic aerosol on the partitioning of inorganic species is studied.

2. MODEL DESCRIPTION

2.1 THE BASELINE ISORROPIA-II MODEL

ISORROPIA-II and its latest version 2.3 (Fountoukis and Nenes, 2007; *http://isorropia.epfl.ch*) is the base model used a starting point for the ISORROPIA-lite development. The current version contains all fixes to bugs identified in earlier versions of ISORROPIA-II (see *http://isorropia.epfl.ch* and Song et al., 2018). The "baseline" ISORROPIA-II model simulation used hereon explicitly calculates the activity coefficients of mixtures and also assumes that the aerosol is always in a stable state, therefore it is solid at RH below the mutual deliquescence RH of its components. The module is tested in the gas-aerosol partitioning ("forward") mode.

2.2 FROM ISORROPIA-II TO ISORROPIA-LITE

ISORROPIA-lite is based on the ISORROPIA-II (Fountoukis and Nenes, 2007) code, hence it treats the thermodynamics of aerosol containing Ca^{2+}, K^+, Mg^{2+}, SO_4^{2-}, Na^+, NH_4^+, NO_3^-, Cl^-, H_2O and their equilibrium with gas-phase HNO_3, NH_3, HCl and H_2O. A series of simplifications that increase computational efficiency have been implemented in ISORROPIA-lite. The aerosol is assumed to be only in a metastable state, so all routines related to the stable state solution (solid+liquid aerosol) from the original code of ISORROPIA-II have been removed. The only solid salt that is allowed to form in ISORROPIA-lite is calcium sulfate ($CaSO_4$), as it is virtually insoluble for most atmospheric humidities and spontaneously precipitates out of solution. The remaining salts that can form are assumed to be completely deliquesced. Further

simplifications address the calculation of binary activity coefficients. In ISORROPIA-II, the coefficients for specific ionic pairs (Kusik and Meissner, 1978) can be computed during runtime or obtained from precalculated tables. In ISORROPIA-lite, only precalculated tables are used. However, the calculation of multicomponent activity coefficients is still done during runtime with the Bromley (1973) method.

ISORROPIA-lite includes one important extension over ISORROPIA-II, in that it allows organic aerosol to perturb the inorganic equilibria by contributing additional aerosol water over that from the inorganic species alone. This organic aerosol water, W_o, is calculated by using the κ hygroscopicity parameter (Petters and Kreidenweis, 2007) based on the relative humidity and the mass of organic compounds within the inorganic aerosol phase:

$$W_o = \frac{\rho_w}{\rho_o} \frac{C_o \kappa}{\left(\frac{1}{RH} - 1\right)}, \quad (1)$$

where ρ_w is the density of water and ρ_o the density, C_o the concentration and κ the hygroscopicity parameter of the organic aerosol. W_o is calculated every time the ISORROPIA-lite solution algorithm requests calculation of aerosol water, and is added to the water computed from the other inorganic components using the Zdanovskii, Stokes, and Robinson (ZSR) equation. This additional aerosol water W_o increases the total aerosol water and tends to slightly elevate the aerosol pH. Both these effects in turn affect the partitioning of the inorganic semi-volatile species. Organic effects on the activity coefficient of inorganic species are not considered because previous work has shown that they are of secondary importance – at least for aerosol pH (e.g., Battaglia et al., 2019; Pye et al., 2020).

ISORROPIA-lite v1.0 can be used to solve the partitioning (forward) problem. The known quantities (inputs) are RH, temperature (T), the organic aerosol concentration, hygroscopicity parameter κ and density and the total (gas+aerosol) concentrations of ammonia, sulfuric acid, sodium, hydrochloric acid, nitric acid, calcium, potassium, and magnesium. The appropriate set of equilibrium equations are solved together with electroneutrality, water activity equations and mass conservation in order to compute the concentrations of species at thermodynamic equilibrium. Details on the thermodynamic properties of the modeled species, the equilibrium reactions and constants and the thermodynamic equilibrium calculations of inorganic species can be found in Fountoukis and Nenes (2007).

2.3 PMCAMX DESCRIPTION AND APPLICATION

PMCAMx is the research version of the publicity available CAMx model (Environ, 2003). It simulates vertical and horizontal advection, vertical and horizontal dispersion, dry and wet deposition and gas, aqueous, and aerosol chemistry. The gas-phase chemical mechanism used here is a modified SAPRC mechanism to account for the VBS treatment of the secondary organic aerosol and it includes 237 reactions of 18 radicals and 91 gases (Carter, 2000; Environ, 2003). The aerosol size and composition distribution is described using 10 size bins with diameters from 40 nm to 40 μm. The model assumes that all particles in each size bin have the same composition. The aerosol species simulated are primary and secondary organics, elemental carbon, crustal species, sodium, chloride, sulfate, nitrate, ammonium, calcium, potassium, magnesium and water. In this application of PMCAMx, we use the bulk equilibrium assumption; therefore the bulk aerosol and gas phases are assumed to be always in equilibrium.

PMCAMx was applied over Europe during May 2008, which is the EUCAARI summer intensive measurement period. The modeling domain, including all of Europe, is a region of 5400 × 5832 km^2. The grid resolution used is 36 × 36 km^2 (24,300 cells per layer) and there are 14 vertical layers with the total height extending up to 6 km above ground level. Inputs to the model such as horizontal wind components, vertical diffusivity, temperature, pressure, water vapor, rainfall, and clouds are provided by the Weather Research and Forecasting (WRF) meteorological model (Skamarock et al., 2008). Land emissions from the GEMS dataset (Visschedijk et al., 2007) and international shipping emissions were included in the anthropogenic gas-phase emissions. Anthropogenic particulate emissions include the elemental and organic carbon emissions (Kulmala et al., 2009) and the urban dust emissions (Kakavas and Pandis, 2021). Biogenic emissions were based on MEGAN (Guenther et al., 2006). Sea-salt emissions were developed using the approach of O'Dowd et al. (2008). More details about the inputs can be found in Fountoukis et al. (2011) and Kakavas and Pandis (2021).

The results of this simulation were used for the online and off-line evaluation of ISORROPIA-lite. Because the thermodynamic calculations in this application of PMCAMx are performed assuming always equilibrium between PM_{10} and the gas phase, the monthly average PM_{10} concentrations of each cell of each atmospheric level of PMCAMx, including ground level, were used to create an input file for off-line ISORROPIA-lite and ISORROPIA-II forward mode simulations. Also for this, the predicted gas concentrations of nitric acid, ammonia, hydrochloric acid and sulfuric acid were added to the particulate phase concentrations together with the simulated RH and temperature. The organic aerosol concentrations are not included at first to focus on the differences between ISORROPIA-lite and ISORROPIA-II from the assumption of aerosol state and binary activity coefficient approach. This test is atmospherically-relevant because it includes atmospheric states encountered over a continental scale, including terrestrial and marine environments.

3. RESULTS AND DISCUSSION

3.1 ISORROPIA-LITE OFF-LINE EVALUATION

3.1.1 Computational requirements

ISORROPIA-lite was first evaluated off-line against ISORROPIA-II in stable mode (with online binary activity coefficients calculation) for a standard set of conditions (***Table 1***). 331,520 tests were performed covering fully the corresponding chemical and meteorological space. All the timing tests were performed on a computer with two Intel Xeon Silver 4110 CPU 2.1 GHz and 64 GB of RAM. ISORROPIA-II required 6.5 CPU s, 52% more than the 4.2 CPU s required by ISORROPIA-lite. Therefore, replacing ISORROPIA-II by ISORROPIA-lite, for these tests at least will result in a reduction of the corresponding computational cost by approximately 35%. Running ISORROPIA-lite using online calculation of binary activity coefficients slowed down the calculations by 26%.

In the second off-line test we used the predictions of PMCAMx at ground level over Europe for May 2008 (European conditions), a total of over 23,000 points as inputs for ISORROPIA-II in stable mode and ISORROPIA-lite. These cases are studied separately because of their relevance to near ground air quality and human health. For this second test ISORROPIA-II required 55% more CPU time than ISORROPIA-lite (0.42 versus 0.27 s). The acceleration of the calculations by ISORROPIA-lite was the same as the first test and equal to 35% of the time required by ISORROPIA-II. The use of the look-up tables of the binary activity coefficients reduced the CPU time by 18% of ISORROPIA-II and the simplification of the metastable state contributed another 17%.

Differences in the frequency of occurrence of conditions suitable for the formation of a stable aerosol state (solid+liquid particles) but also for the activity coefficients calculation at lower temperatures are responsible for the differences in the computational performance of the two thermodynamic models. The higher the frequency of such conditions the higher the computational savings offered by the new module. The calculation of the organic aerosol water has a negligible effect on the computational speed of ISORROPIA-lite (not shown).

3.1.2 Comparison of ISORROPIA-lite against ISORROPIA-II

We use as metrics for the comparison of the predictions of the various models the normalized mean bias (NMB) and the normalized mean error (NME), defined as:

$$NMB_j = \frac{\sum_{i=1}^{n}\left[C_{i,j}^{\text{lite}} - C_{i,j}^{\text{II}}\right]}{\sum_{i=1}^{n} C_{i,j}^{\text{II}}} \quad (2)$$

$$NME_j = \frac{\sum_{i=1}^{n}\left|C_{i,j}^{\text{lite}} - C_{i,j}^{\text{II}}\right|}{\sum_{i=1}^{n} C_{i,j}^{\text{II}}} \quad (3)$$

where $C_{i,j}^{\text{lite}}$ and $C_{i,j}^{\text{II}}$ are the corresponding concentrations of species j predicted by each model for test case i and n is the total number of test cases examined.

The predictions of ISORROPIA-lite (without organic aerosol water) were first compared with those of ISORROPIA-II in stable mode (with online calculation of binary activity coefficients) model for both off-line tests. The discrepancies between the ISORROPIA-lite and ISORROPIA-II predictions for the concentrations of the various semivolatile aerosol components are all less than 25% (***Table 2***). They are lower for chloride and ammonium and higher for nitrate and water. For the gas phase components, they are also less than 25% (***Table 2***). For gas-phase ammonia and hydrochloric acid they are 10% or less and for nitric acid they are less than 25%. These differences are mainly found at low to intermediate RHs, when the stable mode solution contains both a solid and a liquid phase. Please note that for many of these conditions, the metastable solution may reflect better the ambient aerosol state; these discrepancies should therefore not be interpreted as ISORROPIA-lite errors but uncertainty due to its phase state.

For both set of conditions (standard and European), ISORROPIA-lite tends to predict higher amounts of inorganic aerosol and lower concentrations of inorganic

	Na^+ ($\mu g\ m^{-3}$)	H_2SO_4 ($\mu g\ m^{-3}$)	NH_3 ($\mu g\ m^{-3}$)	HNO_3 ($\mu g\ m^{-3}$)	HCl ($\mu g\ m^{-3}$)	Ca^{2+} ($\mu g\ m^{-3}$)	K^+ ($\mu g\ m^{-3}$)	Mg^{2+} ($\mu g\ m^{-3}$)	RH (%)	T (K)
Standard set of conditions[a]										
Min	0.024	0.52	0.28	0.04	0.02	0.003	0.002	0.001	10.6	236
Max	5.4	10.3	13.5	9.2	8.5	0.53	0.33	0.2	96	306
European conditions[b]										
Min	0.06	0.57	0.28	0.06	0.03	0.003	0.002	0.001	12	265
Max	5.4	7.4	13.5	9.1	8.5	0.53	0.33	0.2	96	306

Table 1 Range of concentrations for species in the off-line analysis.

[a] 331,520 tests.

[b] 23,680 tests.

	NH_4^+	Cl^-	H^+	NO_3^-	HNO_3 (g)	HCl (g)	NH_3 (g)	H_2O	Dry PM
ISORROPIA-lite versus ISORROPIA-II (stable mode, online act. coef.)									
Standard set of conditions									
NMB (%)	7.8	8.4	135	24	−22	−6.2	−11	42	4.5
NME (%)	8.2	10	137	24	22	7.5	11	42	4.7
European conditions									
NMB (%)	7.7	3.8	64	13	−21	−4.3	−5.5	13	3.1
NME (%)	8.2	4.2	68	13	21	4.7	5.8	13	3.2
ISORROPIA-II (stable mode, tables) versus ISORROPIA-II (stable mode, online act. coef.)									
Standard set of conditions									
NMB (%)	−0.2	−0.4	1.4	−0.4	0.4	0.3	0.3	−1.5	−0.1
NME (%)	1.4	1.2	12	4.4	4.2	0.9	1.9	2.3	0.8
European conditions									
NMB (%)	−1.6	−0.9	−3.6	−2.5	4.1	1	1.2	−2.1	−0.6
NME (%)	2.5	1.3	9.2	4.1	6.6	1.4	1.8	2.4	1
ISORROPIA-II (metastable mode, online act. coef.) versus ISORROPIA-II (stable mode, online act. coef.)									
Standard set of conditions									
NMB (%)	7.9	8.6	136	24	−22	−6.4	−11	42	4.5
NME (%)	8.1	9.9	137	24	22	7.3	11	42	4.6
European conditions									
NMB (%)	8.7	4.1	65	15	−24	−4.6	−6.2	13	3.5
NME (%)	8.7	4.1	65	15	24	4.6	6.2	13	3.5
ISORROPIA-lite (organic aerosol water presence versus absence)									
Standard set of conditions									
NMB (%)	1.8	3.9	6.7	2.6	−3.9	−3.3	−2.9	12	0.9
NME (%)	1.8	3.9	8.1	2.6	3.9	3.3	2.9	12	0.9
European conditions									
NMB (%)	2.5	2.3	7	2.3	−5.3	−2.8	−2.1	8.2	1
NME (%)	2.5	2.3	8.5	2.3	5.3	2.8	2.1	8.2	1

Table 2 Normalized mean biases and normalized mean errors for the off-line tests.

gases than ISORROPIA-II in stable mode (***Figure 1***). The mean errors are small and range from 4.2% for chloride, to 24% for nitrate. For water, the mean error was 42% for the standard set of conditions and 14% for the European set. The highest discrepancies are found for the hydrogen ion (H^+) predictions (137% for the standard set, 68% for the European ground set), which translates to a pH uncertainty of approximately 0.15 units.

The effect of changing both the binary activity coefficient calculations and metastable state assumption, on the predictions of ISORROPIA-II and the discrepancies with ISORROPIA-lite is quantified one change at a time. The introduction of the pre-calculated tables has a small effect on ISORROPIA-II (stable mode) predictions for both set of conditions with mean errors varying from 1.2% for chloride to 6.6% for nitric acid (***Table 2***). Even for [H^+], the mean error is equal to 12% for the standard set and 9.2% for the European conditions (***Figure 2***). The simplification leads to slightly lower predicted concentrations with biases less than 2.5% for all the major aerosol components and water, and slightly higher concentrations (biases less than 4.1%) for all the inorganic gases. These results strongly suggest that pre-calculated binary activity coefficient tables introduce small errors in both set of conditions and represent a relatively safe way to speed up the calculations.

As expected, the assumption of metastable aerosol for all RH conditions has the largest impact on simulated concentrations. The comparison of a version of ISORROPIA-II which uses the complete activity coefficient module in stable and metastable mode was used for the analysis. For both set of conditions, the normalized mean

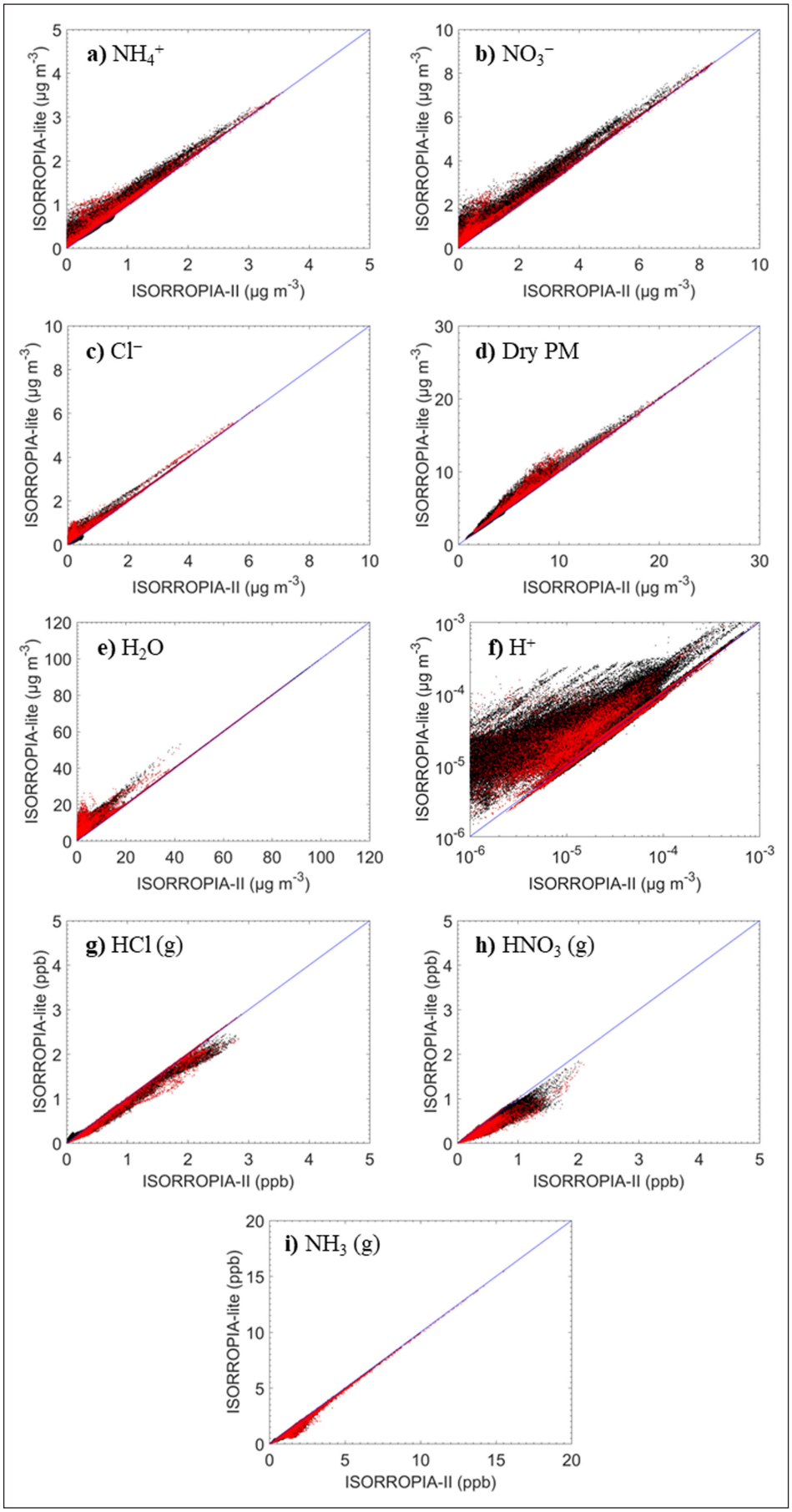

Figure 1 Comparison of the particulate and gas-phase concentrations predicted by ISORROPIA-II in stable mode (with online binary activity coefficients calculation) and ISORROPIA-lite for the off-line simulations for the standard (black) and European (red) set of conditions: **a)** ammonium, **b)** nitrate, **c)** chloride, **d)** dry PM, **e)** water, **f)** hydrogen ion, **g)** hydrochloric acid, **h)** nitric acid, and **i)** ammonia. There are 331,520 points in these graphs.

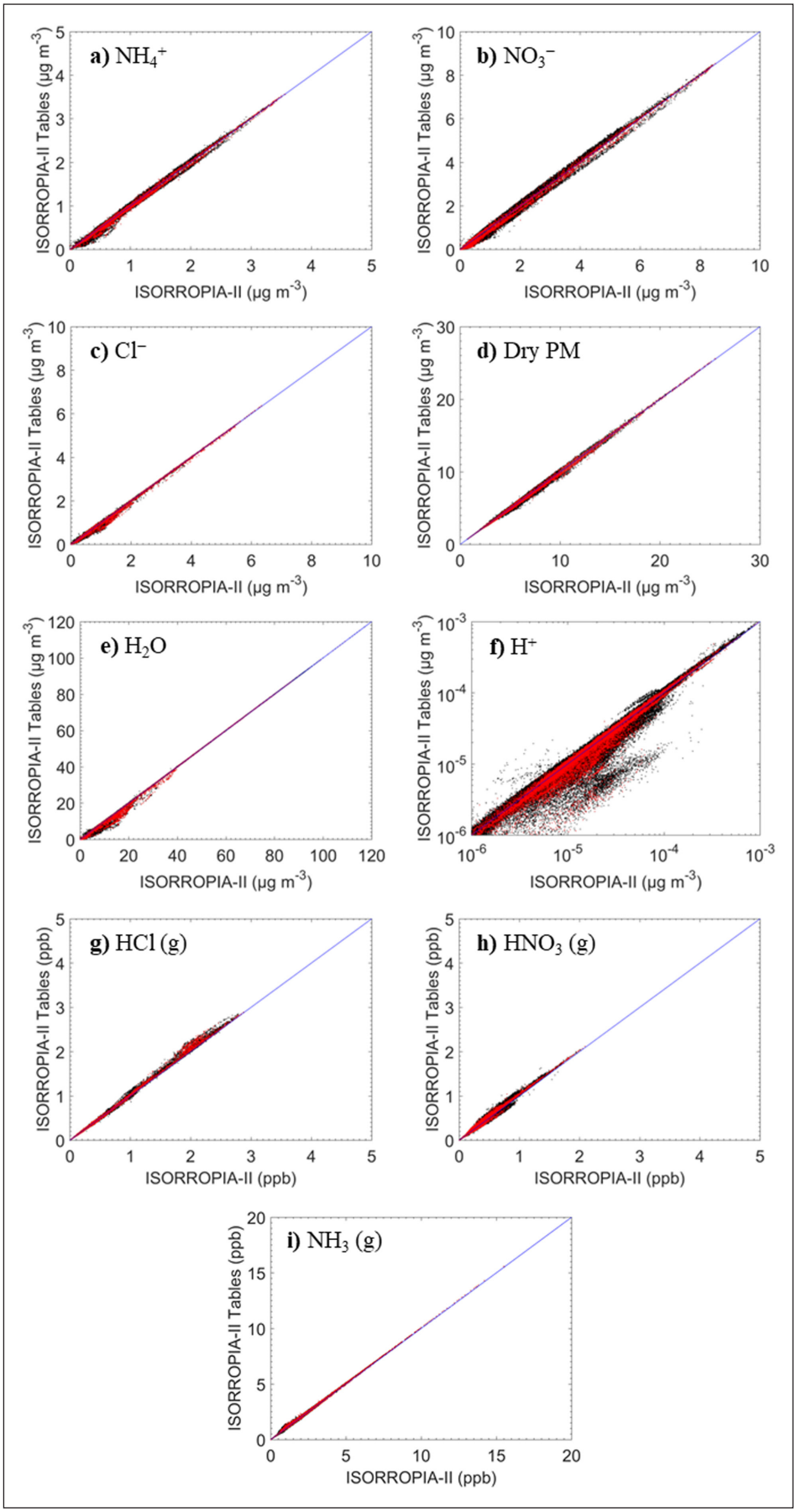

Figure 2 Comparison of the particulate and gas-phase concentrations predicted by ISORROPIA-II in stable mode with online binary activity coefficients calculation and with pre-calculated tables for the off-line simulations for the standard (black) and European (red) set of conditions: **a)** ammonium, **b)** nitrate, **c)** chloride, **d)** dry PM, **e)** water, **f)** hydrogen ion, **g)** hydrochloric acid, **h)** nitric acid, and **i)** ammonia. There are 331,520 points in these graphs.

errors range from 4.1% for chloride to 24% for nitric acid (***Table 2***). Water mean error was equal to 42% for the standard set of conditions and 13% for the European ground conditions. The highest discrepancy (137% for the standard set, 65% for the European set) was found for [H^+] (***Figure 3***). Therefore, the assumed metastable equilibrium state is mainly responsible for the differences of the predictions of the two thermodynamic modules and their respective configuration.

The upper levels of the atmosphere, included in the standard set of conditions, are characterized by lower RHs and temperatures than at ground level – and with it, the frequency where the metastable and stable assumptions differ. In both sets of conditions, the greatest discrepancies were found in water and hydrogen ion levels because the stable state solution of ISORROPIA-II at low RH predicts solid aerosol where water and [H^+] do not exist (and for the sake of comparison were set equal to zero), and ISORROPIA-lite always predicts an aqueous solution.

3.2 ISORROPIA-II VS. ISORROPIA-LITE IN PMCAMX

Figure 4 presents the predicted ground level concentrations of the major inorganic PM components by PMCAMx using ISORROPIA-II in stable mode (with the complete activity coefficient module) and the corresponding changes when ISORROPIA-lite (without organic aerosol water effects) is used.

Sodium and chloride concentrations are higher over the sea, because they are the major components of sea salt, and lower over continental Europe. When ISORROPIA-lite was used for the simulation of aerosol thermodynamics in PMCAMx, predicted sodium and chloride concentrations decreased on average by approximately 0.6%. The low maximum difference of 0.2 μg m^{-3} over the central Mediterranean Sea occurs because metastable state particles have more water, are larger and hence have a higher deposition velocity.

Predicted nitrate concentrations exceed 7 μg m^{-3} over the Netherlands, Belgium, United Kingdom, and northern France, while for the rest of Europe lower concentrations are predicted (up to 3 μg m^{-3}) when ISORROPIA-II in stable mode is used. Using ISORROPIA-lite caused an increase on average nitrate concentration of approximately 10%. More specifically, average nitrate increased up to 0.4 μg m^{-3} over most of continental Europe except Belgium and Netherlands, where an average decrease of 0.1 μg m^{-3} is predicted. In Belgium and Netherlands, nitrate resides mainly in the particulate phase and the RH is generally high enough so that changes in liquid water content have minor impact on nitrate, while in other European locations, changes have a stronger impact.

Ammonium levels up to 3.5 μg m^{-3} are predicted in areas with high nitrate concentrations when ISORROPIA-II in stable mode is used, existing mainly as ammonium sulfate, ammonium nitrate and ammonium chloride. Ammonium increased on average by 2% when we used ISORROPIA-lite. More specifically, average ammonium concentrations increased up to 0.1 μg m^{-3} and decreased by 0.05 μg m^{-3} in the same areas where nitrate did. Compared to nitrate, ammonium in Belgium and the Netherlands resides mainly in the gas-phase. Therefore, in such cases, changes in the liquid water content have minor impact on ammonium (Nenes et al., 2020), while for the rest of Europe a stronger impact emerges.

Sulfate concentrations using ISORROPIA-II in stable mode are high over the Mediterranean and neighboring countries such as Italy and Greece (up to 6 μg m^{-3}), while for the rest of Europe concentrations less than 5 μg m^{-3} are predicted. Using ISORROPIA-lite caused a negligible sulfate decrease over the Mediterranean Sea of 0.02 μg m^{-3} and a negligible increase of 0.01 μg m^{-3} over continental Europe.

Water concentrations are enhanced over the marine areas because of the higher concentrations of hygroscopic sea salt, while over continental Europe are lower. As expected, due to the assumed metastable state of ISORROPIA-lite for low RH values, water concentrations are on average higher than for the ISORROPIA-II simulations by 6.5%. More specifically, an average increase of 1–2.5 μg m^{-3} is predicted over continental Europe, while over the Mediterranean Sea higher increases are predicted (up to 7 μg m^{-3}). The existence of high concentrations of hygroscopic sea salt together with enough RH values below the deliquescence point of NaCl are responsible for the higher increases over the sea.

Hydrochloric acid is predicted to have higher concentrations over water especially in the Mediterranean Sea (up to 0.5 ppb), while in the rest of Europe less than 0.25 ppb are predicted when ISORROPIA-II in stable mode is used (***Figure 5***). Sodium chloride (NaCl), with higher concentrations over the water (e.g., Mediterranean Sea), reacts with the available nitric acid driving some of the existing chloride in the gas-phase. When ISORROPIA-lite is used, average hydrochloric acid concentration decreased by 0.8%, especially over the Mediterranean Sea and northern Italy. The average concentration differences are very low (up to 0.015 ppb in Mediterranean) and occur because the additional water mass, predicted by the metastable state, drove more of the gas phase to partition to the aerosol to satisfy equilibrium.

Nitric acid concentrations are higher over the Mediterranean Sea (up to 2 ppb) than the rest of Europe, where concentrations less than 1 ppb are mostly predicted (***Figure 5***). Using ISORROPIA-lite caused an average decrease of 2%. Average nitric acid concentrations increased by 0.07 ppb over the Belgium, northern Italy and Netherlands, while in the rest of Europe, decreases up to 0.07 ppb are predicted. These results are consistent with the predicted PM nitrate behavior since when there is a decrease of the gas phase concentration, an increase

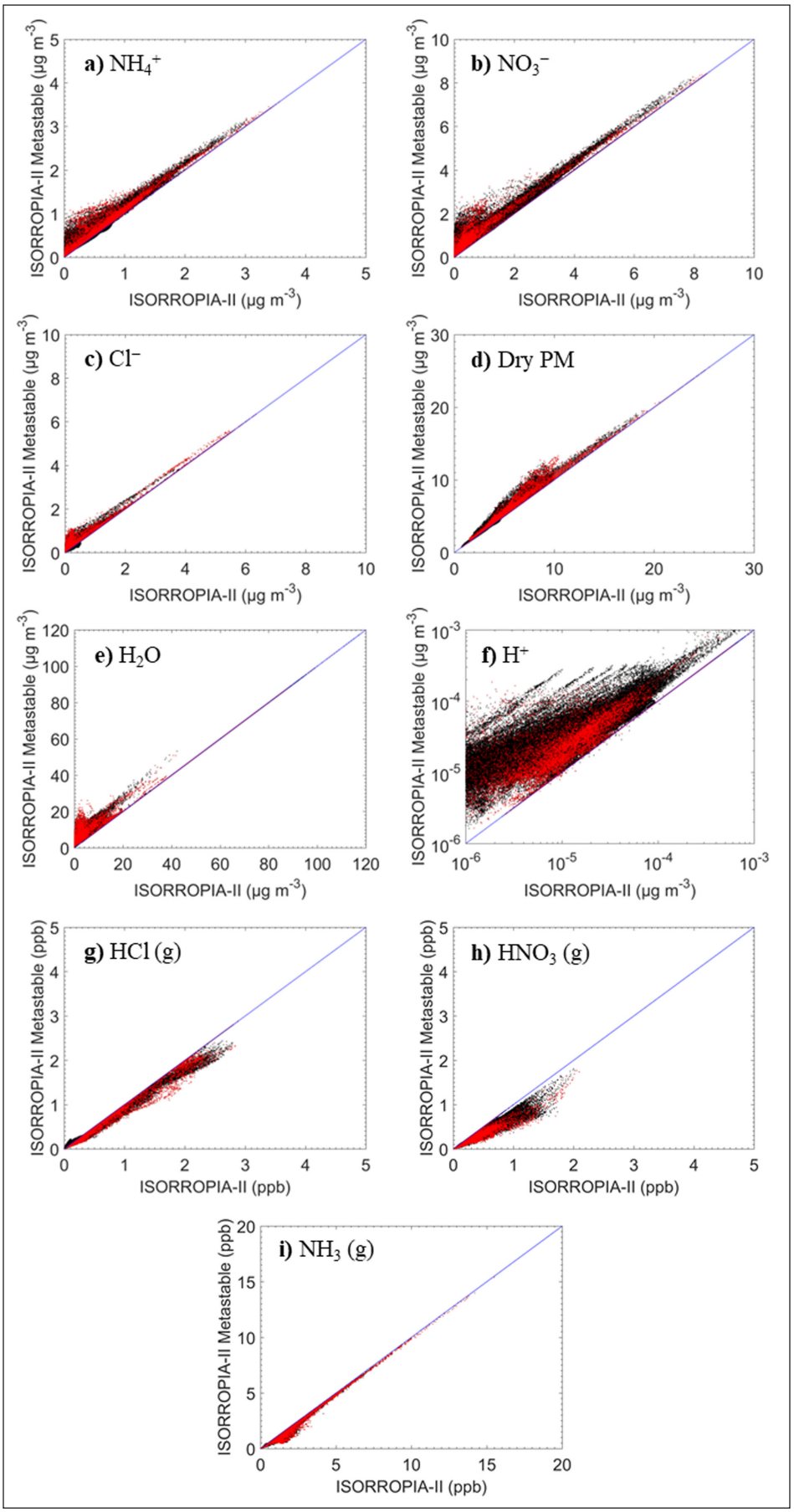

Figure 3 Comparison of the particulate and gas-phase concentrations predicted by ISORROPIA-II (with online binary activity coefficients calculation) in stable and metastable mode for the off-line simulations for the standard (black) and European (red) set of conditions: **a)** ammonium, **b)** nitrate, **c)** chloride, **d)** dry PM, **e)** water, **f)** hydrogen ion, **g)** hydrochloric acid, **h)** nitric acid, and **i)** ammonia. There are 331,520 points in these graphs.

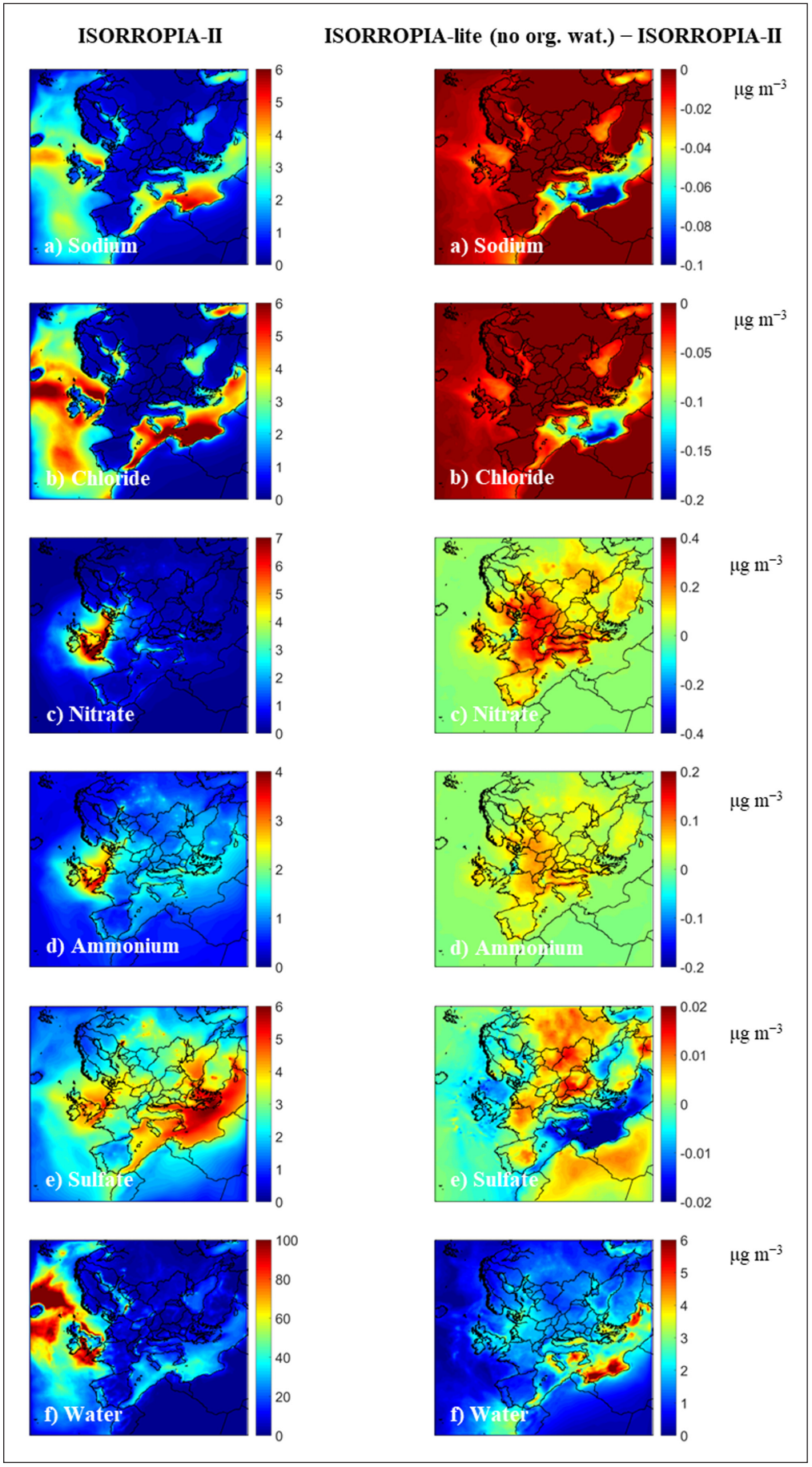

Figure 4 Average ground-level PM_{10} concentrations (in µg m^{-3}) of **a)** sodium, **b)** chloride, **c)** nitrate, **d)** ammonium, **e)** sulfate, and **f)** water using ISORROPIA-II in stable mode with online calculation of binary activity coefficients and ISORROPIA-lite without organic water during May 2008.

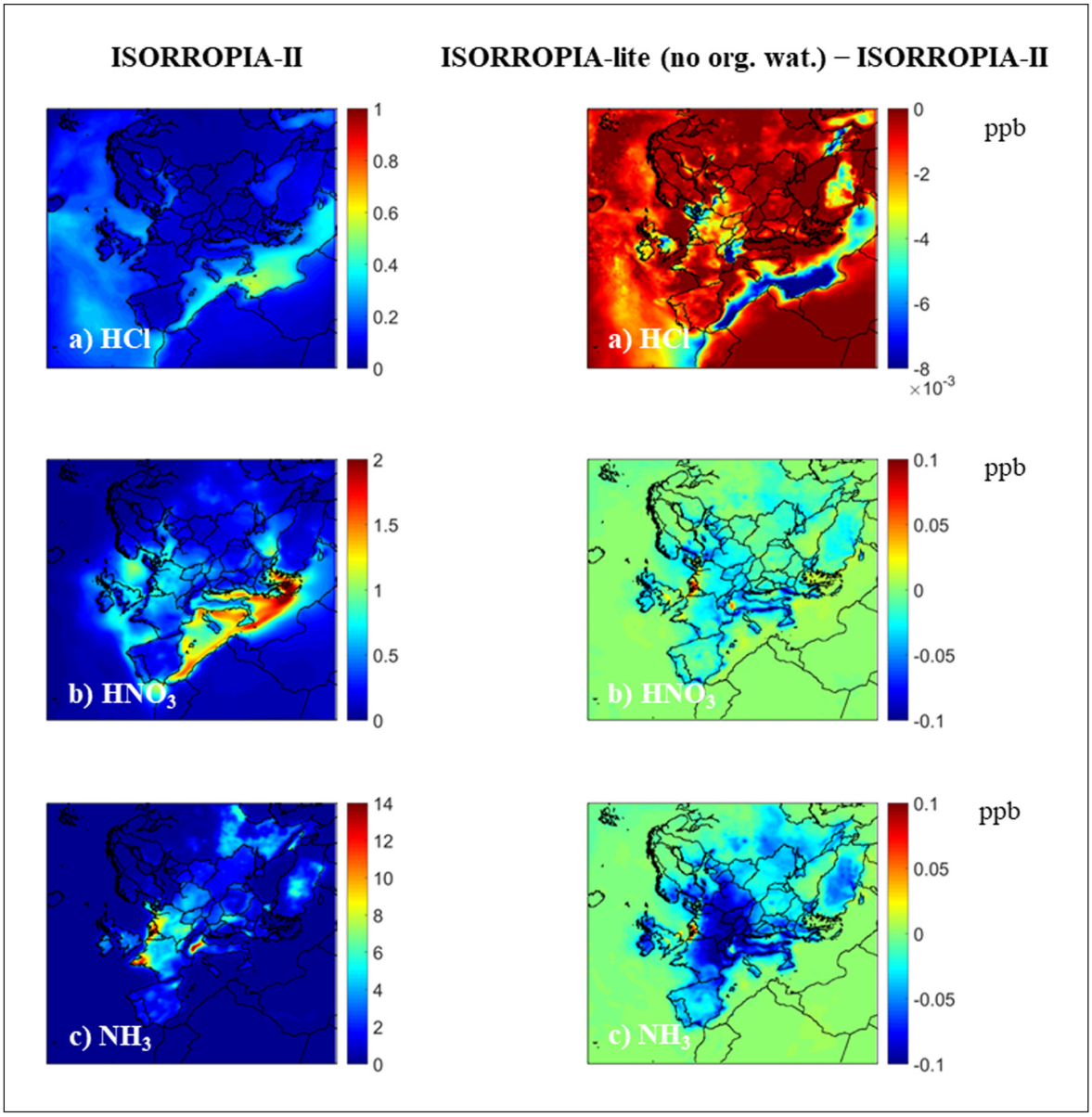

Figure 5 Average predicted ground-level concentrations (in ppb) of **a)** hydrochloric acid, **b)** nitric acid and **c)** ammonia using ISORROPIA-II in stable mode with online calculation of binary activity coefficients and ISORROPIA-lite without organic water during May 2008.

of the particulate phase is predicted and vice versa. Changes in liquid water content have a minor impact on nitric acid levels.

Average ammonia concentrations are higher over Belgium, Netherlands, northern France and northern Italy mainly because of high agricultural emissions (***Figure 5***). When ISORROPIA-lite is used, ammonia decreased by 2% on average. As expected, ammonia increased by 0.07 ppb over Belgium and Netherlands, while in the rest of Europe decreases up to 0.07 ppb are predicted.

The computational time needed for the entire simulation during May 2008 by PMCAMx using ISORROPIA-II in stable mode and with the complete activity coefficient module was 64 CPU h. Using ISORROPIA-lite for the simulation of aerosol thermodynamics in PMCAMx reduced the required computational time by approximately 6 CPU h (9% reduction).

In general, the higher levels of aerosol water associated with the metastable state drive more of the semi-volatile gases to the aerosol to satisfy equilibrium. However, there are places such as Belgium and the Netherlands with high enough RH values, where nitrate resides mainly in the particulate and ammonium in the gas-phase, so that the changes in liquid water content have a minor impact (Nenes et al., 2020). Nevertheless, the average predicted concentration differences between ISORROPIA-II and ISORROPIA-lite are minor for all inorganic species in the aerosol phase.

3.3 THE EFFECTS OF ORGANIC WATER ON THE THERMODYNAMIC SOLUTION

3.3.1 Effects for equilibrium partitioning of PM_{10}

For the calculation of the organic aerosol water in ISORROPIA-lite we assumed that secondary organic

aerosol (SOA) constitutes the only hygroscopic component of organic aerosol, with a hygroscopicity parameter κ equal to 0.15 and density equal to 1 g cm^{-3} (Cerully et al., 2015). Predictions of ISORROPIA-lite with and without the effects of organic aerosol water were first evaluated off-line (***Figure 6***). The differences of the concentrations of the semivolatile aerosol components are on average less than 5% (***Table 2***). For both set of conditions, the presence of organic aerosol water leads to higher amounts of inorganic aerosol and lower concentrations of inorganic gases. The additional water mass of the organic aerosol drives more of the gas phase to partition to the aerosol to satisfy equilibrium. The mean differences are small, ranging from 1.8% for ammonium to 5.3% for nitric acid. The additional organic aerosol water is on average 12% of the inorganic for the standard set of conditions and 8% for the European. For hydrogen ion (H^+), the predicted concentration differences correspond up to 0.05 pH units. Similar low pH differences also occur when we assume that the organic water is additive and affects pH without feedbacks on inorganic semivolatiles (e.g., Bougiatioti et al., 2016).

The predicted ground level concentrations of the major inorganic PM components by PMCAMx using ISORROPIA-lite when the organic aerosol water is absent in the simulations and the corresponding changes when is present are shown in ***Figure 7***. As expected, sulfate is not affected by the presence of the additional water mass of the organic aerosol. Sodium concentrations, when the organic aerosol water is present in the simulation, decreased on average by approximately 0.2% due to the increase of the dry deposition rate. Some of the chloride deposited together with sodium, but the presence of additional organic aerosol water over the sea drove more of the gas phase to the aerosol. Therefore, chloride concentrations increased on average by 0.3% with a maximum negligible difference of 0.02 μg m^{-3} over southern Atlantic. Predicted nitrate concentrations increased on average by approximately 4%. More specifically, nitrate increased over continental Europe by 0.25 μg m^{-3} with highest average increases over Belgium, northern France, and Netherlands. Ammonium increased on average by approximately 1% when the organic aerosol water is present in the simulation with average concentration increases up to 0.08 μg m^{-3} in the same areas where nitrate did.

Hydrochloric acid concentrations in the presence of the additional water mass decreased on average by 1.5%, especially over the sea part of Europe, where average decreases of approximately 0.01 ppb are predicted (***Figure 8***). Nitric acid concentrations when the organic aerosol water is present in the simulation as expected decreased on average by 1%. Average nitric acid concentrations decreased by 0.04 ppb over the Belgium, Italy and Netherlands, while in the rest of Europe small decreases up to 0.03 ppb are predicted (***Figure 8***). Ammonia concentrations decreased on average by 0.9%. More specifically, ammonia decreased by 0.1 ppb over Belgium, northern France and Netherlands, while in the rest of Europe decreases up to 0.08 ppb are predicted (***Figure 8***). The results are consistent with the predicted PM behavior since when there is a decrease of the gas phase concentration, an increase of the particulate phase is predicted and vice versa.

As expected, due to the additional water mass of the organic aerosol, water concentration increased on average by 8% over the modeling domain with an average increase of 1-4 μg m^{-3} over continental Europe and 8 μg m^{-3} over the Atlantic sea. The additional water mass is mostly in the fine fraction since it is related to secondary organic aerosol water which has condensed mostly on the accumulation mode.

3.3.2 Effects on PM_1 aerosol

In this section we focus on PM_1 instead of PM_{10} because the most important effects of the organic water are expected in this size range. The predicted ground level PM_1 concentrations by PMCAMx using ISORROPIA-lite when the organic aerosol water is absent in the simulations and the corresponding changes when it is present are shown in ***Figure 9***. Fine sodium decreased over the sea on average by approximately 1% when the organic aerosol water is present in the simulation due to the size increase of particles caused by the additional organic water. Fine chloride concentrations increased on average by 3% with a maximum negligible difference of 0.005 μg m^{-3} over continental Europe. Predicted PM_1 nitrate and ammonium concentrations increased on average by 6% and 1% respectively when the organic aerosol water is present in the simulation with the same absolute concentration increases of these of PM_{10}, while PM_1 sulfate decreased on average by less than 0.1% with a maximum negligible difference of 0.005 μg m^{-3} over continental Europe and Atlantic ocean. The additional organic aerosol water increased fine water concentrations on average by 29%.

Together with average changes we also focus on the temporal variation of the effects on four sites (Paris, Melpitz, Cabauw, and Finokalia) with different characteristics (***Table 3***). The PM_1 water concentrations in all sites are quite variable ranging from close to zero to above 100 μg m^{-3} when the RH approaches 100% (***Figure 10***). The presence of organic aerosol water as expected increased PM_1 water concentrations in all sites. Water increases of a few μg m^{-3} are predicted during most of the days and sites. During the high RH periods PM_1 water increased up to 35 μg m^{-3} in Cabauw and Finokalia, 40 μg m^{-3} in Melpitz and 100 μg m^{-3} in Paris (not shown).

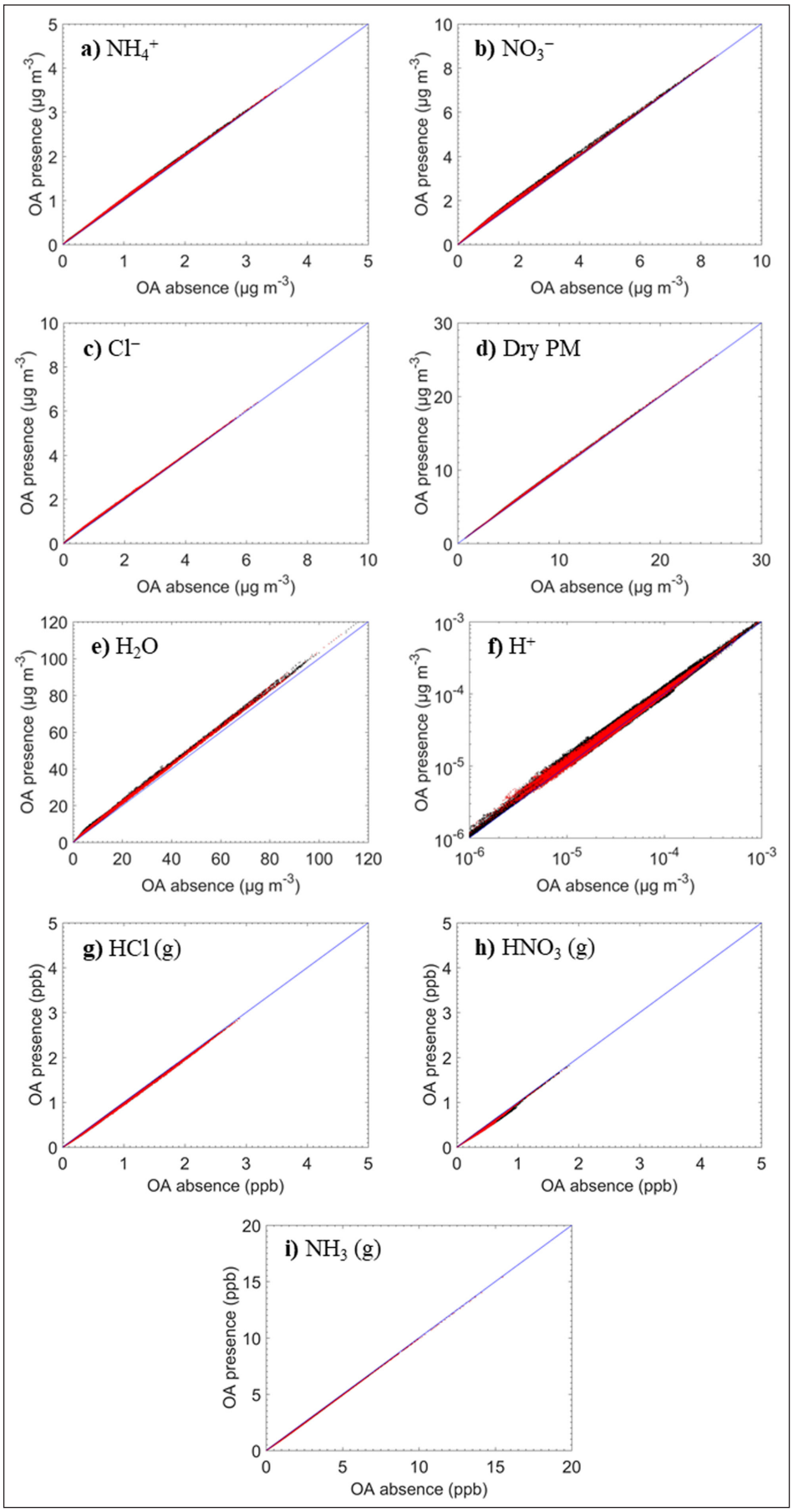

Figure 6 Comparison of the particulate and gas-phase concentrations predicted by ISORROPIA-lite when the organic aerosol water is present and absent for the off-line simulations for the standard (black) and European (red) set of conditions: **a)** ammonium, **b)** nitrate, **c)** chloride, **d)** dry PM, **e)** water, **f)** hydrogen ion, **g)** hydrochloric acid, **h)** nitric acid, and **i)** ammonia. There are 331,520 points in these graphs.

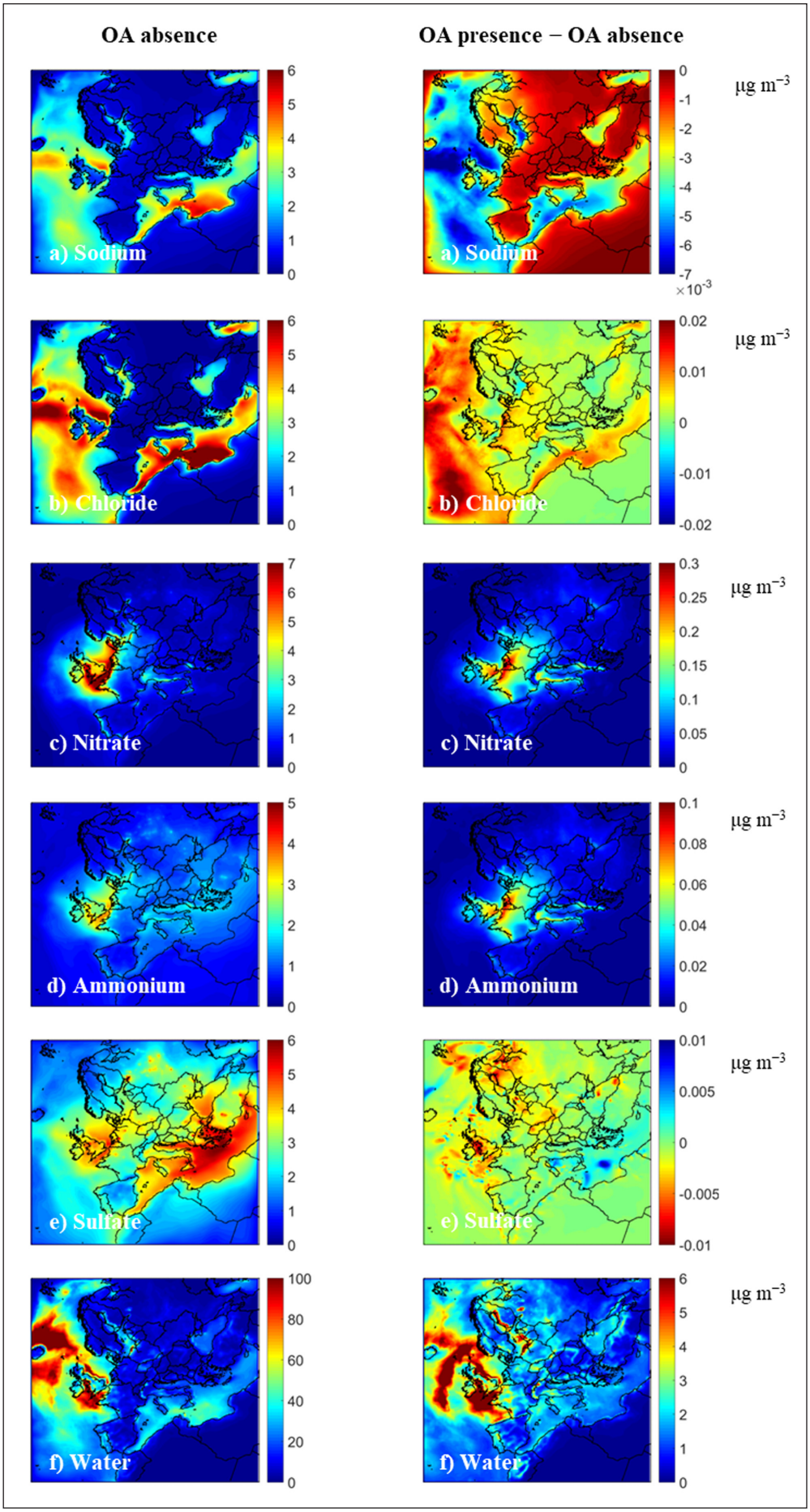

Figure 7 Average ground-level PM_{10} concentrations (in μg m^{-3}) of **a)** sodium, **b)** chloride, **c)** nitrate, **d)** ammonium, **e)** sulfate, and **f)** water using ISORROPIA-lite when the organic aerosol water is absent and present in the simulation during May 2008.

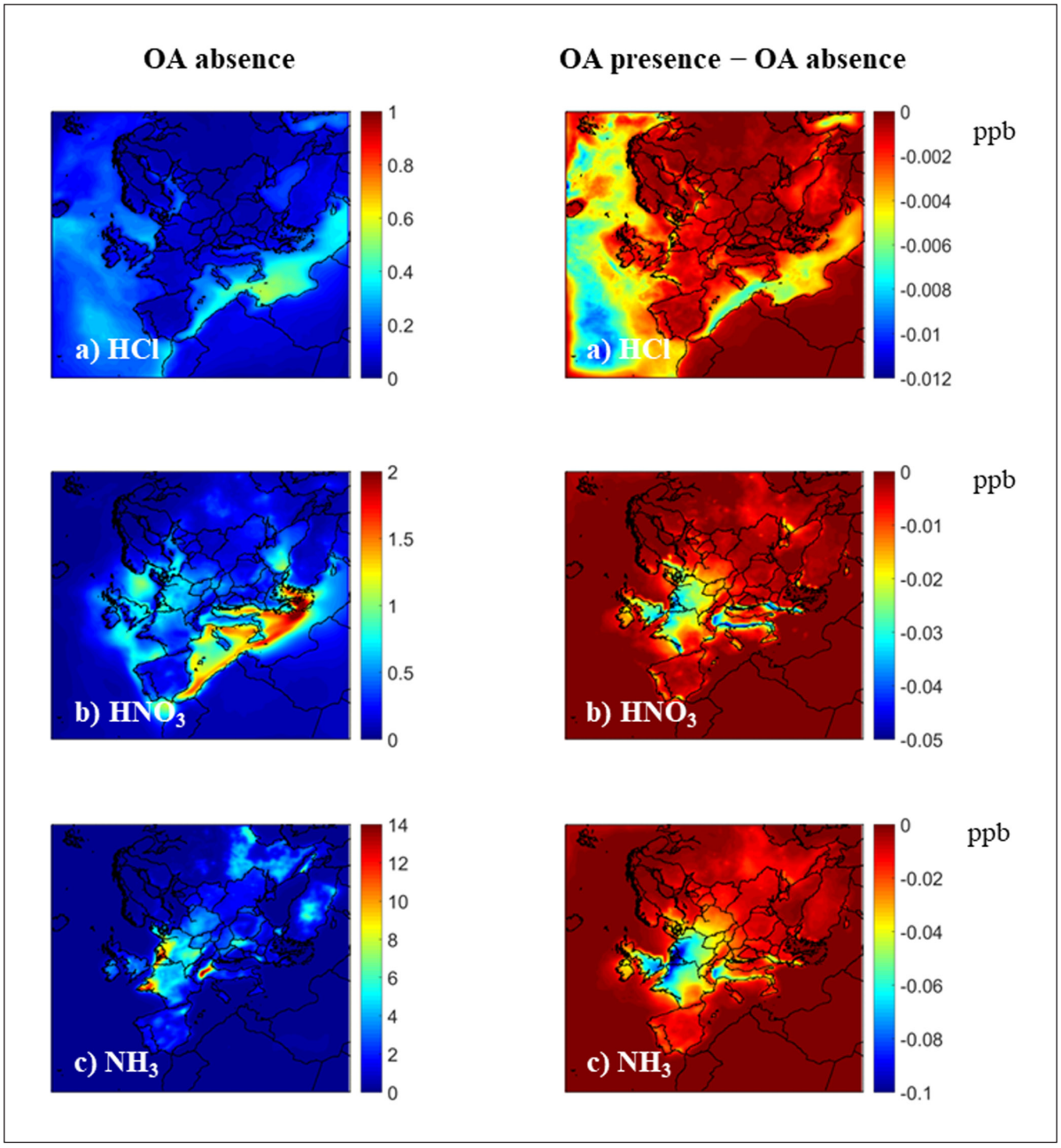

Figure 8 Average predicted ground-level concentrations (in ppb) of **a)** hydrochloric acid, **b)** nitric acid and **c)** ammonia using ISORROPIA-lite when the organic aerosol water is absent and present in the simulation during May 2008.

For PM_1 nitrate, concentrations up to 10 μg m^{-3} are predicted in Cabauw, up to 2 μg m^{-3} in Finokalia, and up to 7 μg m^{-3} in Melpitz and Paris (***Figure 11***). The presence of the additional water mass affected PM_1 nitrate especially in Cabauw, where increases up to 0.7 μg m^{-3} are predicted during most of the time and up to 1 μg m^{-3} during the last day of the month. As for Cabauw, increases up to 0.7 μg m^{-3} occurred in Melpitz and Paris, while fine nitrate in Finokalia did not change during most of the time with the exception of a couple of periods during which changes of 0.1 μg m^{-3} are predicted.

Fine ammonium concentrations reach values of approximately 5 μg m^{-3} in Cabauw, 2.5 μg m^{-3} in Finokalia, 4 μg m^{-3} in Melpitz, and 3 μg m^{-3} in Paris during May 2008 (***Figure 12***). When the organic water effects are considered, PM_1 ammonium concentrations increase up to 0.3 μg m^{-3} for Cabauw, Melpitz, and Paris, while in Finokalia, PM_1 ammonium is virtually unaffected. The increases occurred at the same time the corresponding ones of fine nitrate did.

Temporal profiles of PM_1 components during the simulation period indicated that secondary organic aerosol water could contribute to the total PM_1 aerosol water content and influence fine nitrate and ammonium concentrations especially at nighttime. Fine chloride concentrations are not expected to change significantly with time, especially in the examined sites (characterized by low chloride levels), affected by the organic aerosol

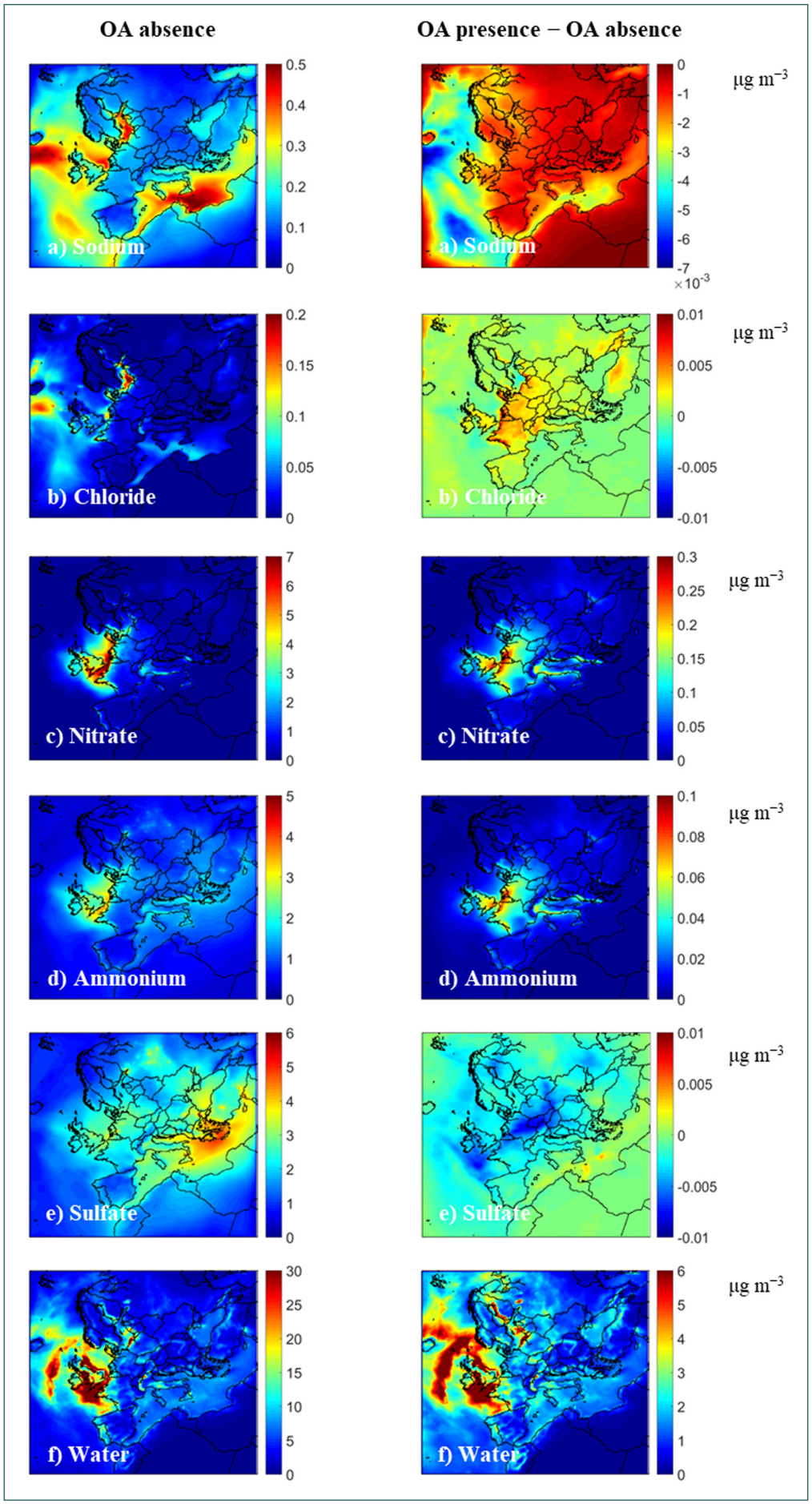

Figure 9 Average ground-level PM_1 concentrations (in µg m^{-3}) of **a)** sodium, **b)** chloride, **c)** nitrate, **d)** ammonium, **e)** sulfate, and **f)** water using ISORROPIA-lite when the organic aerosol water is absent and present in the simulation during May 2008.

SITE	TYPE OF SITE	SOA LEVELS	AMMONIUM LEVELS	NITRATE LEVELS	SULFATE LEVELS	RH LEVELS	LOCATION IN EUROPE
Finokalia, Greece	Remote	High	Modest	Low	High	High	South
Cabauw, Netherlands	Rural	High	High	High	High	High	North
Melpitz, Germany	Rural	High	Modest	High	High	High	North
Paris, France	Urban	High	Modest	High	High	High	West

Table 3 Characteristics of the four selected sites.

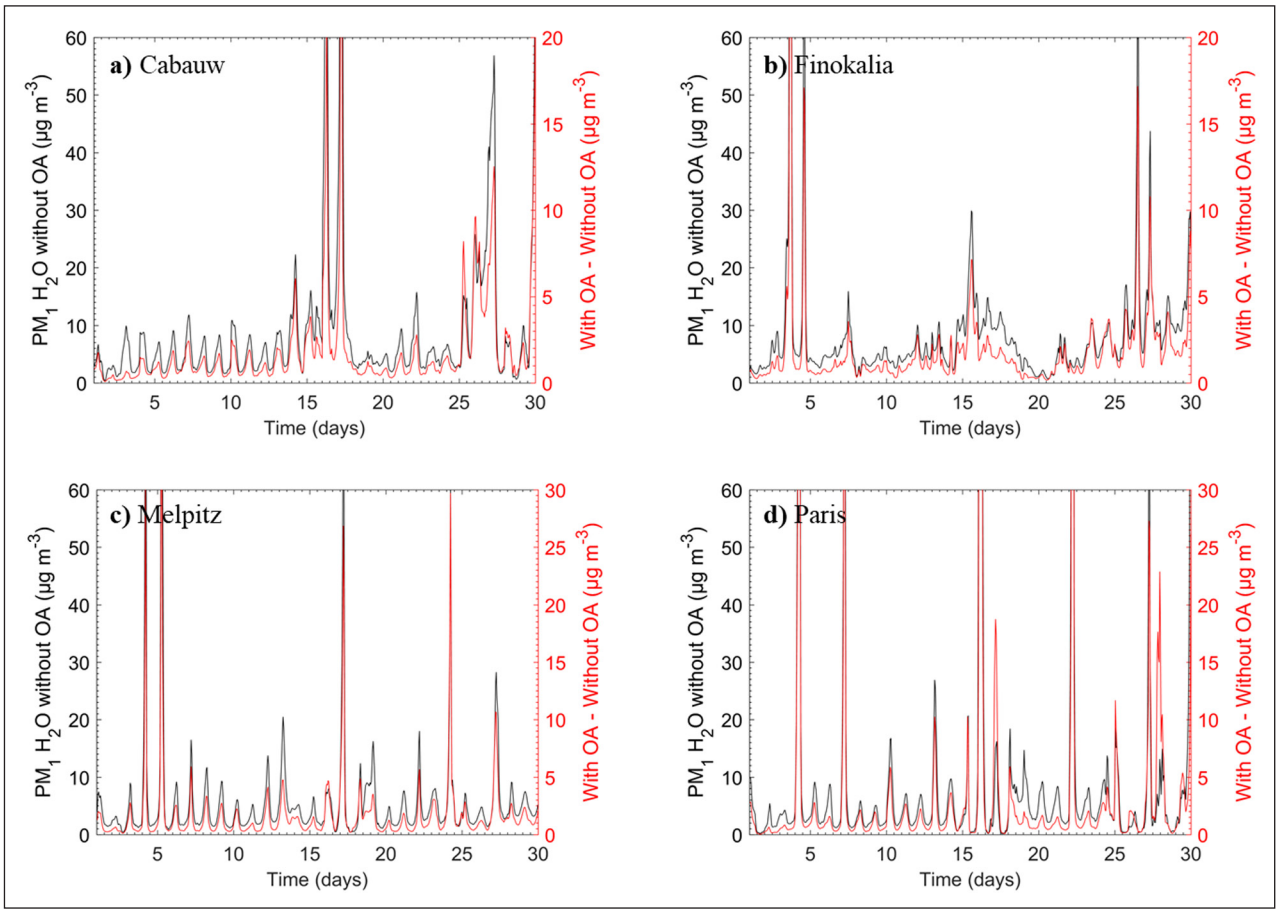

Figure 10 PM_1 water concentration (in μg m^{-3}) when the organic aerosol water is absent (black) and the corresponding concentration difference when is present (red) in the simulation for **a)** Cabauw, Netherlands; **b)** Finokalia, Greece; **c)** Melpitz, Germany; and **d)** Paris, France during May 2008.

water. However, they could be affected in other locations – especially urban environments during biomass burning periods, where organic compounds and chloride salts can constitute a considerable fraction of submicron aerosol (Metzger et al., 2006; Fountoukis et al., 2009; Gunthe et al., 2021).

4. CONCLUSIONS

ISORROPIA-lite, a computationally efficient aerosol equilibrium module for large-scale models that treats the thermodynamics of Na^+– NH_4^+– SO_4^{2-}– NO_3^-– Cl^-– Ca^{2+}– K^+– Mg^{2+}– Organics– H_2O aerosol systems is developed. The new module is based on ISORROPIA-II version 2.3 with extensions to include the effects of organic water uptake on inorganic partitioning. To increase computational speed and reduce code size, ISORROPIA-lite assumes that the aerosol is always in metastable equilibrium and precalculated tables are used for the binary activity coefficients. Compared to ISORROPIA-II, ISORROPIA-lite is 35% faster and accelerates PMCAMx 3D simulations by approximately 10%.

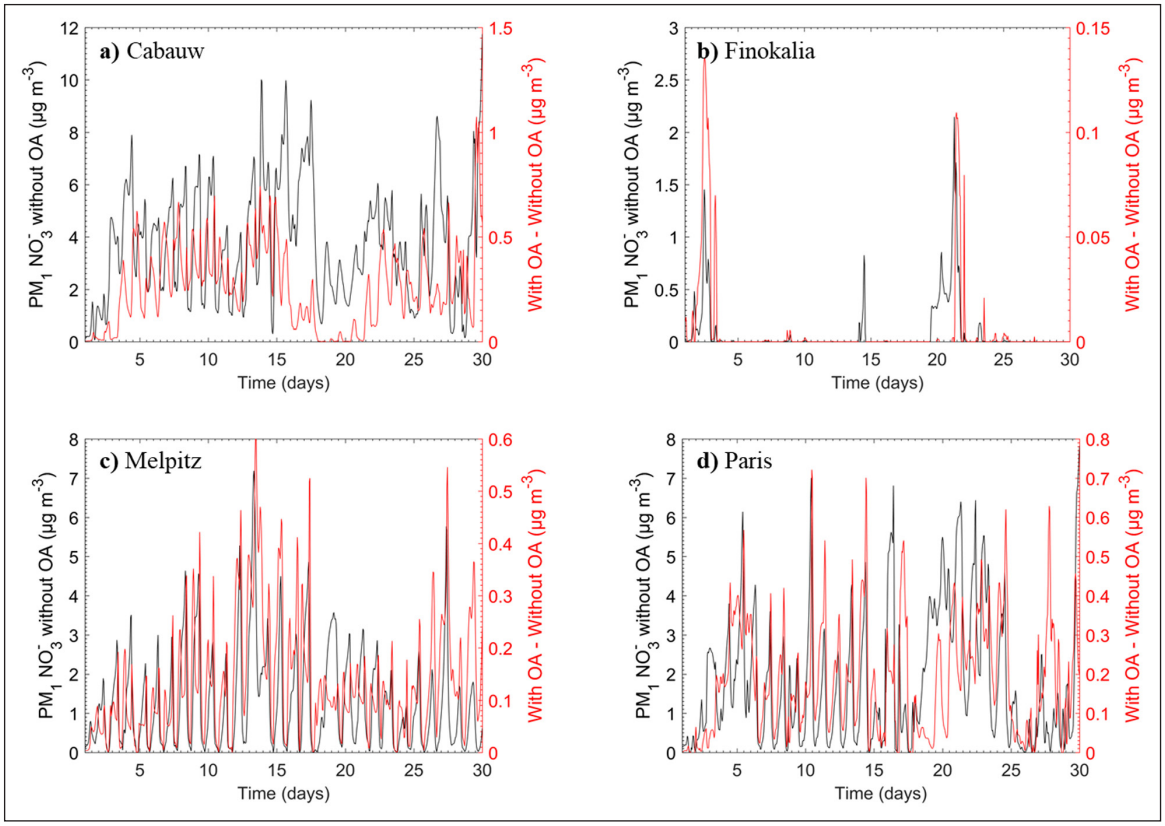

Figure 11 PM_1 nitrate concentration (in μg m^{-3}) when the organic aerosol water is absent (black) and the corresponding concentration difference when is present (red) in the simulation for **a)** Cabauw, Netherlands; **b)** Finokalia, Greece; **c)** Melpitz, Germany; and **d)** Paris, France during May 2008.

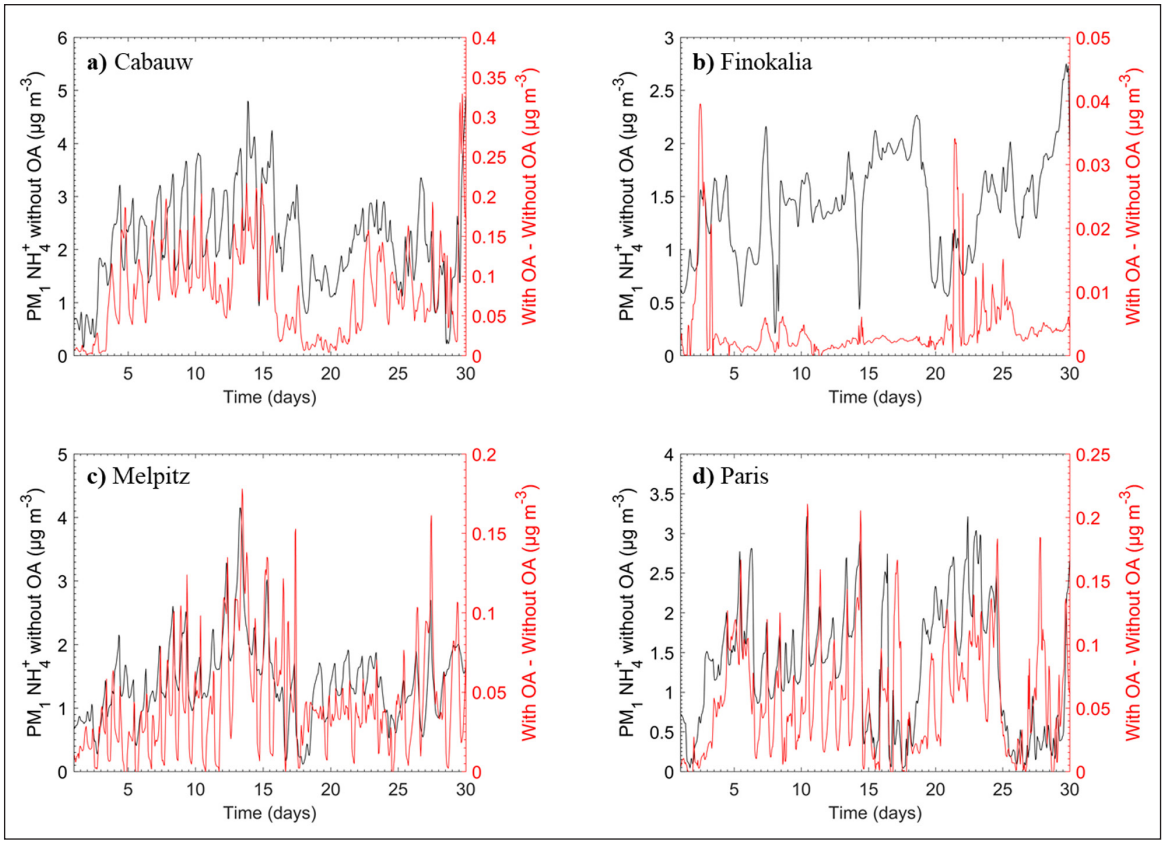

Figure 12 PM_1 ammonium concentration (in μg m^{-3}) when the organic aerosol water is absent (black) and the corresponding concentration difference when is present (red) in the simulation for **a)** Cabauw, Netherlands; **b)** Finokalia, Greece; **c)** Melpitz, Germany; and **d)** Paris, France during May 2008.

In terms of composition, for the partitioning (forward) problem, the discrepancies between ISORROPIA-lite (without organic aerosol water) and ISORROPIA-II (stable mode) predictions for the concentrations of the various semivolatile aerosol components were generally low (less than 25%) in the off-line tests. In PMCAMx, the results indicated that the major aerosol species concentrations agree to within 10%. Most of these differences in the predictions of the two modules were found at the low to intermediate RH range. However, these discrepancies should not be viewed as errors of ISORROPIA-lite, since in some cases the metastable state may be closer to truth.

Considering organic aerosol water effects in ISORROPIA-lite simulations increased the concentrations of total PM_1 water, nitrate and ammonium and decreased the corresponding gas phase of inorganic semivolatiles since the additional water mass drives more of the gas phase components to partition to the aerosol to satisfy equilibrium. Temporal profiles indicated that organic aerosol water could contribute to the total aerosol water content and increase fine nitrate (up to 1 μg m^{-3}) and ammonium (up to 0.3 μg m^{-3}) concentrations especially at nighttime in places characterized by high RH and organic aerosol levels. On a domain and simulation average the changes were of the order of 30% for fine water and a few percent for the major inorganic aerosol components in the simulated period. The effects of the organic aerosol water in aerosol partitioning in other periods and areas will be the topic of future work with ISORROPIA-lite.

CODE AND DATA AVAILABILITY

The ISORROPIA-lite v1.0 thermodynamic equilibrium code is available at *https://isorropia.epfl.ch* (last access: April 2021, Nenes, 2021). The data in the study is available from the authors upon request.

ACKNOWLEDGEMENTS

This work was supported by the project FORCeS funded from the European Union's Horizon 2020 research and innovation programme under grant agreement No 821205. We also acknowledge support by the project PyroTRACH (ERC-2016-COG) funded from H2020-EU.1.1. – Excellent Science – European Research Council (ERC), project ID 726165.

COMPETING INTERESTS

The authors have no competing interests to declare.

AUTHOR AFFILIATIONS

Stylianos Kakavas *orcid.org/0000-0002-9634-0856*
Institute of Chemical Engineering Sciences, Foundation for Research and Technology Hellas, Patras, Greece; Department of Chemical Engineering, University of Patras, Patras, Greece

Spyros N. Pandis *orcid.org/0000-0001-8085-9795*
Institute of Chemical Engineering Sciences, Foundation for Research and Technology Hellas, Patras, Greece; Department of Chemical Engineering, University of Patras, Patras, Greece

Athanasios Nenes *orcid.org/0000-0003-3873-9970*
Institute of Chemical Engineering Sciences, Foundation for Research and Technology Hellas, Patras, Greece; School of Architecture, Civil and Environmental Engineering, École Polytechnique Fédérale de Lausanne (EPFL), Switzerland

REFERENCES

Amundson, NR, Caboussat, A, He, JW, Martynenko, AV, Savarin, VB and **co-authors.** 2006. A new inorganic atmospheric aerosol phase equilibrium model (UHAERO). *Atmos. Chem. Phys.* 6: 975–992. DOI: *https://doi.org/10.5194/acp-6-975-2006*

Ansari, AS and **Pandis, SN.** 1999a. Prediction of multicomponent inorganic atmospheric aerosol behavior. *Atmos. Environ.* 33: 745–757. DOI: *https://doi.org/10.1016/S1352-2310(98)00221-0*

Ansari, AS and **Pandis, SN.** 1999b. An analysis of four models predicting the partitioning of semivolatile inorganic aerosol components. *Aerosol Sci. Technol.* 31: 129–153. DOI: *https://doi.org/10.1080/027868299304200*

Ansari, AS and **Pandis, SN.** 2000a. Water absorption by secondary organic aerosol and its effect an inorganic aerosol behavior. *Environ. Sci. Technol.* 34: 71–77. DOI: *https://doi.org/10.1021/es990717q*

Ansari, AS and **Pandis, SN.** 2000b. The effect of metastable equilibrium states on the partitioning of nitrate between the gas and aerosol phases. *Atmos. Environ.* 34: 157–168. DOI: *https://doi.org/10.1016/S1352-2310(99)00242-3*

Baker, A, Kanakidou, M, Nenes, A, Croot, PL, Ito, A and **co-authors.** 2021. Changing atmospheric acidity as a modulator of ocean biogeochemistry. *Sci. Adv.* in review. DOI: *https://doi.org/10.5194/egusphere-egu2020-19425*

Bassett, M and **Seinfeld, JH.** 1983. Atmospheric equilibrium model of sulfate and nitrate aerosols. *Atmos. Environ.* 17: 2237–2252. DOI: *https://doi.org/10.1016/0004-6981(83)90221-4*

Battaglia, MA, Jr., Weber, RJ, Nenes, A and **Hennigan, CJ.** 2019. Effects of water-soluble organic carbon on aerosol pH. *Atmos. Chem. Phys.* 19: 14607–14620. DOI: *https://doi.org/10.5194/acp-19-14607-2019*

Bentsen, M, Bethke, I, Debernard, JB, Iversen, T, Kirkevåg, A and **co-authors.** 2013. The Norwegian Earth System Model, NorESM1-M – Part 1: Description and basic evaluation of the physical climate. *Geosci. Model Dev.* 6: 687–720. DOI: *https://doi.org/10.5194/gmd-6-687-2013*

Bertram, AK, Martin, ST, Hanna, SJ, Smith, ML, Bodsworth, A and **co-authors.** 2011. Predicting the relative humidities of liquid-liquid phase separation, efflorescence, and deliquescence of mixed particles of ammonium sulfate, organic material, and water using the organic-to-sulfate mass ratio of the particle and the oxygen-to-carbon elemental ratio of the organic component. *Atmos. Chem. Phys.* 11: 10995–11006. DOI: *https://doi.org/10.5194/acp-11-10995-2011*

Bougiatioti, A, Nikolaou, P, Stavroulas, I, Kouvarakis, G, Weber, R and **co-authors.** 2016. Particle water and pH in the eastern Mediterranean: source variability and implications for nutrient availability. *Atmos. Chem. Phys.* 16: 4579–4591. DOI: *https://doi.org/10.5194/acp-16-4579-2016*

Bromley, LA. 1973. Thermodynamic properties of strong electrolytes in aqueous solutions. *AIChE J.* 19: 313–320. DOI: *https://doi.org/10.1002/aic.690190216*

Brooks, SD, Garland, RM, Wise, ME, Prenni, AJ, Cushing, M and **co-authors.** 2003. Phase changes in internally mixed maleic acid/ammonium sulfate aerosols. *J. Geophys. Res.* 108: 4487–4497. DOI: *https://doi.org/10.1029/2002JD003204*

Brooks, SD, Wise, ME, Cushing, M and **Tolbert, MA.** 2002. Deliquescence Behavior of Organic/Ammonium Sulfate Aerosol. *Geophys. Res. Lett.* 29: 23-1–23-4. DOI: *https://doi.org/10.1029/2002GL014733*

Burgos, M, Andrews, E, Titos, G, Alados-Arboledas, L, Baltensperger, U and **co-authors.** 2019. A global view on the effect of water uptake on aerosol particle light scattering. *Scientific Data*, 6. DOI: *https://doi.org/10.1038/s41597-019-0158-7*

Burgos, MA, Andrews, E, Titos, G, Benedetti, A, Bian, H and **co-authors.** 2020. A global model–measurement evaluation of particle light scattering coefficients at elevated relative humidity. *Atmos. Chem. Phys.* 20: 10231–10258. DOI: *https://doi.org/10.5194/acp-20-10231-2020*

Capaldo, KP, Pilinis, C and **Pandis, SN.** 2000. A computationally efficient hybrid approach for dynamic gas/aerosol transfer in air quality models. *Atmos. Environ.* 34: 3617–3627. DOI: *https://doi.org/10.1016/S1352-2310(00)00092-3*

Carter, WPL. 2000. Documentation of the SAPRC-99 Chemical Mechanism for VOC Reactivity Assessment. *Report to California Air Resources Board*, Contracts No. 92–329 and 95–308.

Cerully, KM, Bougiatioti, A, Hite, JR, Jr., Guo, H, Xu, L, Ng, NL and **co-authors.** 2015. On the link between hygroscopicity, volatility, and oxidation state of ambient and water-soluble aerosols in the southeastern United States. *Atmos. Chem. Phys.* 15: 8679–8694. DOI: *https://doi.org/10.5194/acp-15-8679-2015*

Environ. 2003. User's guide to the comprehensive air quality model with extensions (CAMx), version 4.02, report, ENVIRON Int. Corp., Novato, California, USA.

Fountoukis, C and **Nenes, A.** 2007. ISORROPIA II: a computationally efficient thermodynamic equilibrium model for K^+-Ca^{2+}-Mg^{2+}-NH_4^+-Na^+-SO_4^{2-}-NO_3^--Cl^--H_2O aerosols. *Atmos. Chem. Phys.* 7: 4639–4659. DOI: *https://doi.org/10.5194/acp-7-4639-2007*

Fountoukis, C, Nenes, A, Sullivan, A, Weber, R, Van Reken, T and **co-authors.** 2009. Thermodynamic characterization of Mexico city aerosol during MILAGRO 2006. *Atmos. Chem. Phys.* 9: 2141–2156. DOI: *https://doi.org/10.5194/acp-9-2141-2009*

Fountoukis, C, Racherla, PN, Denier Van Der Gon, HAC, Polymeneas, P, Charalampidis, PE and **co-authors.** 2011. Evaluation of a three-dimensional chemical transport model (PMCAMx) in the European domain during the EUCAARI May 2008 campaign. *Atmos. Chem. Phys.* 11: 10331–10347. DOI: *https://doi.org/10.5194/acp-11-10331-2011*

Guenther, A, Karl, T, Harley, P, Wiedinmyer, C, Palmer, PI and **co-authors.** 2006. Estimates of global terrestrial isoprene emissions using MEGAN (Model of Emissions of Gases and Aerosols from Nature). *Atmos. Chem. Phys.* 6: 3181–3210. DOI: *https://doi.org/10.5194/acp-6-3181-2006*

Gunthe, SS, Liu, P, Panda, U, Raj, SS, Sharma, A and **co-authors.** 2021. Enhanced aerosol particle growth sustained by high continental chlorine emission in India. *Nat. Geosci.* 14: 77–84. DOI: *https://doi.org/10.1038/s41561-020-00677-x*

Guo, H, Liu, J, Froyd, KD, Roberts, JM, Veres, PR and **co-authors.** 2017. Fine particle pH and gas–particle phase partitioning of inorganic species in Pasadena, California, during the 2010 CalNex campaign. *Atmos. Chem. Phys.* 17: 5703–5719. DOI: *https://doi.org/10.5194/acp-17-5703-2017*

Guo, H, Otjes, R, Schlag, P, Kiendler-Scharr, A, Nenes, A and **co-authors.** 2018. Effectiveness of ammonia reduction on control of fine particle nitrate. *Atmos. Chem. Phys.* 18: 12241–12256. DOI: *https://doi.org/10.5194/acp-18-12241-2018*

Guo, H, Xu, L, Bougiatioti, A, Cerully, KM, Capps, SL and **co-authors.** 2015. Fine-particle water and pH in the southeastern United States. *Atmos. Chem. Phys.* 15: 5211–5228. DOI: *https://doi.org/10.5194/acp-15-5211-2015*

Hazeleger, W, Wang, X, Severijns C, Ştefănescu, S, Bintanja, R and **co-authors.** 2011. EC-Earth V2.2: Description and validation of a new seamless earth system prediction model. *Clim. Dyn.* 39: 2611–2629. DOI: *https://doi.org/10.1007/s00382-011-1228-5*

Heitzenberg, J. 1989. Fine particles in the global troposphere: a review. *Tellus*, 41B: 149–160. DOI: *https://doi.org/10.1111/j.1600-0889.1989.tb00132.x*

Iversen, T, Bentsen, M, Bethke, I, Debernard, JB, Kirkevåg, A and **co-authors.** 2013. The Norwegian Earth System Model, NorESM1-M – Part 2: Climate response and scenario projections. *Geosci. Model Dev.* 6: 389–415. DOI: *https://doi.org/10.5194/gmd-6-389-2013*

Jacobson, MZ. 1999. Studying the effect of calcium and magnesium on size-distributed nitrate and ammonium with EQUISOLV II. *Atmos. Environ.* 33: 3635–3649. DOI: *https://doi.org/10.1016/S1352-2310(99)00105-3*

Jathar, SH, Mahmud, A, Barsanti, KC, Asher, WE, Pankow, JF and **co-authors.** 2016. Water uptake by organic aerosol and its influence on gas/particle partitioning of secondary organic aerosol in the United States. *Atmos. Environ.* 129: 142–154. DOI: *https://doi.org/10.1016/j.atmosenv.2016.01.001*

Jin, X, Wang, Y, Li, Z, Zhang, F, Xu, W and **co-authors.** 2020. Significant contribution of organics to aerosol liquid water content in winter in Beijing, China. *Atmos. Chem. Phys*. 20: 901–914. DOI: *https://doi.org/10.5194/acp-20-901-2020*

Kakavas, S and **Pandis, SN.** 2021. Effects of urban dust emissions on fine and coarse PM levels and composition. *Atmos. Environ*. 246: 118006. DOI: *https://doi.org/10.1016/j.atmosenv.2020.118006*

Kakavas, S, Patoulias, D, Zakoura, M, Nenes, A and **Pandis, SN.** 2021. Size-resolved aerosol pH over Europe during summer. *Atmos. Chem. Phys*. 21: 799–811. DOI: *https://doi.org/10.5194/acp-21-799-2021*

Karydis, VA, Tsimpidi, AP, Pozzer, A, Astitha, M and **Lelieveld, J.** 2016. Effects of mineral dust on global atmospheric nitrate concentrations. *Atmos. Chem. Phys*. 16: 1491–1509. DOI: *https://doi.org/10.5194/acp-16-1491-2016*

Kim, YP and **Seinfeld, JH.** 1995. Atmospheric gas – aerosol equilibrium III. Thermodynamics of crustal elements Ca^{2+}, K^{+}, and Mg^{2+}. *Aerosol Sci. Technol*. 22: 93–110. DOI: *https://doi.org/10.1080/02786829408959730*

Kirkevåg, A, Iversen, T, Seland, Ø, Hoose, C, Kristjánsson, JE and **co-authors.** 2013. Aerosol–climate interactions in the Norwegian Earth System Model – NorESM1-M. *Geosci. Model Dev*. 6: 207–244. DOI: *https://doi.org/10.5194/gmd-6-207-2013*

Koo, B, Metzger, S, Vennam, P, Emery, C, Wilson, G and **co-authors.** 2020. Comparing the ISORROPIA and EQSAM Aerosol Thermodynamic Options in CAMx. In: Mensink, C, Gong, W and Hakami, A (eds.), *Air Pollution Modeling and its Application XXVI*. ITM 2018. Springer Proceedings in Complexity, Springer, Cham. DOI: *https://doi.org/10.1007/978-3-030-22055-6_16*

Kulmala, M, Asmi, A, Lappalainen, HK, Carslaw, KS, Poschl, U and **co-authors.** 2009. Introduction: European Integrated Project on Aerosol Cloud Climate and Air Quality interactions (EUCAARI) – integrating aerosol research from nano to global scales. *Atmos. Chem. Phys*. 9: 2825–2841. DOI: *https://doi.org/10.5194/acp-9-2825-2009*

Kusik, C and **Meissner, H.** 1978. Electrolyte activity coefficients in inorganic processing. *AICHE Sym. S*. 74: 14–20.

Meng, ZY, Seinfeld, JH, Saxena, P and **Kim, YP.** 1995. Atmospheric gas – aerosol equilibrium IV. Thermodynamics of carbonates. *Aerosol Sci. Technol*. 23: 131–154. DOI: *https://doi.org/10.1080/02786829508965300*

Metzger, S, Abdelkader, M, Steil, B and **Klingmüller, K.** 2018. Aerosol water parameterization: long-term evaluation and importance for climate studies. *Atmos. Chem. Phys*. 18: 16747–16774. DOI: *https://doi.org/10.5194/acp-18-16747-2018*

Metzger, S, Dentener, F, Krol, M, Jeuken, A and **Lelieveld, J.** 2002b. Gas/aerosol partitioning: 2. Global modeling results. *J. Geophys. Res*. 107: 4313. DOI: *https://doi.org/10.1029/2001JD001103*

Metzger, S, Dentener, F, Pandis, S and **Lelieveld, J.** 2002a. Gas/aerosol partitioning: 1. A computationally efficient model. *J. Geophys. Res*. 107: 4312. DOI: *https://doi.org/10.1029/2001JD001102*

Metzger, S, Mihalopoulos, N and **Lelieveld, J.** 2006. Importance of mineral cations and organics in gas-aerosol partitioning of reactive nitrogen compounds: case study based on MINOS results. *Atmos. Chem. Phys*. 6: 2549–2567. DOI: *https://doi.org/10.5194/acp-6-2549-2006*

Metzger, S, Steil, B, Abdelkader, M, Klingmüller, K, Xu, L and **co-authors.** 2016. Aerosol water parameterisation: a single parameter framework. *Atmos. Chem. Phys*. 16: 7213–7237. DOI: *https://doi.org/10.5194/acp-16-7213-2016*

Moya, M, Fountoukis, C, Nenes, A, Matias, E and **Grutter, M.** 2007. Predicting diurnal variability of fine inorganic aerosols and their gas-phase precursors near downtown Mexico City. *Atmos. Chem. Phys*. 7: 11257–11294. DOI: *https://doi.org/10.5194/acpd-7-11257-2007*

National Research Council (NRC). 2012. A National Strategy for Advancing Climate Modeling, Washington, DC: The National Academies Press. DOI: *https://doi.org/10.17226/13430*

Nenes, A, Pandis, SN, Pilinis, C. 1998. ISORROPIA: A new thermodynamic equilibrium model for multiphase multicomponent inorganic aerosols. *Aquat. Geochem*. 4: 123–152. DOI: *https://doi.org/10.1023/A:1009604003981*

Nenes, A, Pandis, SN, Weber, RJ and **Russell, A.** 2020. Aerosol pH and liquid water content determine when particulate matter is sensitive to ammonia and nitrate availability. *Atmos. Chem. Phys*. 20: 3249–3258. DOI: *https://doi.org/10.5194/acp-20-3249-2020*

Nenes, A, Pilinis, C and **Pandis, SN.** 1999. Continued development and testing of a new thermodynamic aerosol module for urban and regional air quality models. *Atmos. Environ*. 33: 1553–1560. DOI: *https://doi.org/10.1016/S1352-2310(98)00352-5*

O'Dowd, CD, Langmann, B, Varghese, S, Scannell, C, Ceburnis, D and **co-authors.** 2008. A combined organic-inorganic sea-spray source function. *Geophys. Res. Lett*. 35: L01801. DOI: *https://doi.org/10.1029/2007GL030331*

Parsons, MT, Knopf, DA and **Bertram, AK.** 2004. Deliquescence and crystallization of ammonium sulfate particles internally mixed with water-soluble organic compounds. *J. Phys. Chem. A*, 108: 11600–11608. DOI: *https://doi.org/10.1021/jp0462862*

Peckhaus, A, Grass, S, Treuel, L and **Zellner, R.** 2012. Deliquescence and Efflorescence Behavior of Ternary Inorganic/Organic/Water Aerosol Particles. *J. Phys. Chem. A* 116: 6199–6210. DOI: *https://doi.org/10.1021/jp211522t*

Petters, MD and **Kreidenweis, SM.** 2007. A single parameter representation of hygroscopic growth and cloud condensation nucleus activity. *Atmos. Chem. Phys*. 7: 1961–1971. DOI: *https://doi.org/10.5194/acp-7-1961-2007*

Pilinis, C, Capaldo, KP, Nenes, A and **Pandis, SN.** 2000. MADM– a new multicomponent aerosol dynamics model. *Aerosol Sci. Tech*. 32: 482–502. DOI: *https://doi.org/10.1080/027868200303597*

Pilinis, C and **Seinfeld, JH.** 1987. Continued development of a general equilibrium model for inorganic multicomponent atmospheric aerosols. *Atmos. Environ*. 21: 2453–2466. DOI: *https://doi.org/10.1016/0004-6981(87)90380-5*

Pye, HOT, Nenes, A, Alexander, B, Ault, AP, Barth, MC and **co-authors.** 2020. The Acidity of Atmospheric Particles and Clouds. *Atmos. Chem. Phys*. 20: 4809–4888. DOI: *https://doi.org/10.5194/acp-20-4809-2020*

Roeckner, E, Bauml, G, Bonaventura, L, Brokopf, R, Esch, M and **co-authors.** 2003. The Atmospheric General Circulation Model ECHAM5. Part I: Model Description. MPI Report 349, Max Planck Institute for Meteorology, Hamburg, Germany, 127.

Rood, MJ, Shaw, MA, Larson, TV and **Covert, DS.** 1989. Ubiquitous nature of ambient metastable aerosol. *Nature*. 337: 537–539. DOI: *https://doi.org/10.1038/337537a0*

Skamarock, WC, Klemp, JB, Dudhia, J, Gill, DO, Barker, DM and **co-authors.** 2008. *A Description of the Advanced Research WRF Version 3*. NCAR Tech. Note NCAR/TN–475+STR, 113.

Song, S, Gao, M, Xu, W, Shao, J, Shi, G and **co-authors.** 2018. Fine-particle pH for Beijing winter haze as inferred from different thermodynamic equilibrium models. *Atmos. Chem. Phys*. 18: 7423–7438. DOI: *https://doi.org/10.5194/acp-18-7423-2018*

Song, S, Nenes, A, Gao, M, Zhang, Y, Liu, P and **co-authors.** 2019. Thermodynamic Modeling Suggests Declines in Water Uptake and Acidity of Inorganic Aerosols in Beijing Winter Haze Events during 2014/2015–2018/2019. *Environ. Sci. Technol. Lett*., 6: 752–760. DOI: *https://doi.org/10.1021/acs.estlett.9b00621*

Tang, IN, Fung, KH, Imre, DG and **Munkelwitz, HR.** 1995. Phase transformation and metastability of hygroscopic microparticles. *Aerosol Sci. Technol*., 23: 443–453. DOI: *https://doi.org/10.1080/02786829508965327*

Tilgner, A, Schaefer, T, Alexander, B, Barth, M, Collett, JL, Jr. and **co-authors.** 2021. Acidity and the multiphase chemistry of atmospheric aqueous particles and clouds. *Atmos. Chem. Phys. Discuss*., 21: 13483–13536. DOI: *https://doi.org/10.5194/acp-2021-58*

Visschedijk, AJH, Zandveld, P and **Denier van der Gon, HAC.** 2007. TNO Report 2007 A-R0233/B: A high resolution gridded European emission database for the EU integrated project GEMS, Netherlands, Organization for Applied Scientific Research.

Wexler, AS and **Clegg, SL.** 2002. Atmospheric aerosol models for systems including the ions H^+, NH_4^+, Na^+, SO_4^{2-}, NO_3^-, Cl^-, Br^-, and H_2O. *J. Geophys. Res*. 107: 4207. DOI: *https://doi.org/10.1029/2001JD000451*

Wexler, AS and **Seinfeld, JH.** 1991. Second-generation inorganic aerosol model. *Atmos. Environ*., 25A: 2731–2748. DOI: *https://doi.org/10.1016/0960-1686(91)90203-J*

TO CITE THIS ARTICLE:
Kakavas, S, Pandis, SN and Nenes, A. (2022). ISORROPIA-Lite: A Comprehensive Atmospheric Aerosol Thermodynamics Module for Earth System Models. *Tellus B: Chemical and Physical Meteorology*, 74(2022), 1–23. DOI: *https://doi.org/10.16993/tellusb.33*

Submitted: 14 February 2022 Accepted: 14 February 2022 Published: 25 March 2022